

DESIGN AND TEST OF A ROCKET MOTOR
EXPANSION JOINT

Thesis by

Lt. Cmdr. R. L. Reiserer U.S.N.
Lt. K. P. Barden U.S.N.

In Partial Fulfillment of the Requirements for
the Professional Degree in Aeronautical Engineering.

California Institute of Technology

Pasadena, California

1947

ACKNOWLEDGMENT

In presenting this thesis, the authors wish to express their appreciation and gratitude to Dr. E. E. Sechler and Dr. L. G. Dunn of the Guggenheim Aeronautical Laboratory, California Institute of Technology, and to Mr. Frank Denison of the California Institute of Technology Jet Propulsion Laboratory, for their supervision, helpful suggestions, and assistance in carrying out the research.

TABLE OF CONTENTS

<u>Subject</u>	<u>Page</u>
Summary	1
I Introduction	3
II Equipment and Test Procedure	5
III Discussion of Results	9
IV Recommendation for Future Studies	15
V References	16
VI Index to Tables	17
VII Index to Figures	17
VIII Index to Photographs	17

SUMMARY

The purpose of this investigation was to carry on the work of investigating stresses encountered in the design of rocket motor expansion joints. The previous work was done on a semi-circular expansion joint by Commander N. J. Kleiss, U.S.N., and Lt. Comdr. S. W. Kerkering, U.S.N. in a thesis submitted to the Aeronautics Department of the California Institute of Technology.

Information was desired to make possible a more favorable design. The problem consists of continuing the investigation on a different design, thereby determining a trend for future designs.

The design chosen was a semicircular ring shell with reversed curvatures of the edges. It was felt that this configuration would eliminate most of the bending stresses found present at the weld of the semicircular design, and would make possible a more even distribution of stresses throughout the expansion joint.

Because the stresses encountered were so far beyond the elastic limit of the material, even for small total elongations of the expansion joint, no theoretical solutions of the problem were possible.

An analysis of the curves and data shows the joint to be unsatisfactory, particularly from the viewpoint of withstanding the internal pressure. Since the previous work indicated that the internal pressure was not critical for the semicircular design, it seems that a compromise of the two designs would more satisfactorily meet the requirements of withstanding both

the elongation and the internal pressure.

An alternate design has been indicated which will make possible a trend of designs that should lead to a solution.

INTRODUCTION

If the science of guided missiles is to continue to advance, each component part of the missile must be perfected. This means that a satisfactory propulsive system capable of continual operation to some degree must be developed. The development of a satisfactory expansion joint for the rocket motor is one phase of this problem.

The expansion joint must withstand internal pressures up to 600 p.s.i., and must be capable of large repeated elongations. The difference in temperature between the inner and outer shells causes relative expansions and contractions which must be absorbed by an expansion joint. The external dimensions of the expansion joint are usually dictated by aerodynamic considerations, while the internal dimensions are determined to a great extent by the fuel flow requirements. Further considerations in design are weight, simplicity of design, ease of production, and maintenance.

Figure A shows the combustion chamber, cooling chamber, and expansion joint of a typical rocket motor. Fuel under high pressure is pumped through the cooling chamber and acts as a coolant for the combustion chamber. High combustion temperatures cause elongation of both the inner and outer shells. However, because the temperature of the inner shell is several hundred degrees higher than that of the outer shell, the elongations are not equal. Consequently, an expansion joint that will allow the outer shell to expand with the inner shell without imposing too

severe loads on the latter is required. The elongation of the rocket motor with the temperature distribution as shown in Figure A is of the order of 0.10" in ten inches. This indicates that for a motor of a given length two or three expansion joints may be required.

The tests on the specimens were planned to give: a) the stresses at critical positions on the expansion joint at various internal pressures and elongations, b) the elongation and loadings which would give permanent set, and c) the number of repeated elongations necessary to cause failure.

Four specimens of the same design but of various thicknesses were tested. The first two specimens were 0.028 and 0.035 inches thick respectively. The third and fourth were both from 0.053 to 0.057" thick. The specimens were manufactured by a spinning process in which a piece of flat sheet was spun down over a wooden mandrel while hot. This made accurate control of the thicknesses almost impossible. It was originally intended that two of the specimens be 0.04" and two be 0.05" thick in order that comparisons could be made between this and the semicircular design of Ref. 4. However, during the fabrication of the first set of specimens, the standard sheet stock used (0.0418 and 0.0538) was decreased in thickness so much that the first two specimens mounted were useless except as introductions to the problems ahead and as preliminary indications of where the critical stresses occurred.

II

EQUIPMENT AND TEST PROCEDURE

Fig. B illustrates the method of assembling the expansion joint on the pressure vessel. The entire assembly was manufactured of mild steel (1020) and assembled by welding. The first specimen was 0.028" in thickness, the second 0.035, and the third and fourth each from 0.053 to 0.057. The desired internal pressures were obtained by pumping oil through a 5/8" pipe threaded hole at one end of the cylinder. A Blackhawk hydraulic jack was used to supply the pressure. Pressure readings were taken from a large, dial type, N.A.C.A., hydraulic gage.

Depending on whether the specimen was in tension or compression, either two steel bars or two steel plugs were screwed into the centers of the top and bottom plates of the pressure vessel. (See Photograph #3).

A Tinius Olsen beam balance testing machine was used to apply the tension or compression and to control the elongation. (See Photographs 1 and 2.). The force measuring components of this machine were very good, however trouble was encountered in trying to obtain a given elongation at a constant internal pressure in the specimen.

Spherical bearings were used in tension tests and ball bearing pyramids in compression tests in order to apply a centralized load without end moments.

Values of stress were obtained by means of SR-4, type A-8, Baldwin Locomotive electric wire resistance strain gages. Six gages were mounted on the first specimen and eleven on the

second specimen. The locations of attachment are illustrated in Fig. C. On specimen III, eight gages were used, and on specimen IV ten gages were applied. Their locations are also shown in Figure C. On all specimens the gages were located radially at 90° quadrants in order to obtain average readings.

The strain gages were used in conjunction with a multiple channel Wheatstone Bridge designed and made at the California Institute of Technology. Voltage measurement was made by a Leeds and Northrop Potentiometer. This apparatus was capable of measuring the change in voltage in the strain gages to an accuracy of 0.001-millivolt, which corresponds to an accuracy of 12.95 P.S.I. of stress or 0.037% of the proportional limit strain.

The over-all elongation of the specimen was measured by means of a dial gage mounted between the working platforms of the Tinius Olsen machine. This gage measured elongations within 0.001" accuracy.

The first expansion joint specimen tested revealed the need for strain gage calibration well beyond the elastic limit of the material. Therefore, a curve of stress vs. millivolts was obtained in the following manner.

Standard 0.5", flat, pin-ended tensile test specimens were made of the same material used in the manufacture of the expansion joints. Electric strain gages were mounted on opposite sides of the specimens so as to eliminate the effects of any bending. These tensile test specimens were used to obtain the data and curve shown in Table 1 and Figure 1 respectively.

This curve made it possible to convert all millivolt

readings directly to stress values without the use of gage constants. These stresses were used for the final plotting of σ vs. δ .

Specimen I (thickness = 0.028") was too thin to withstand the required internal pressure and was also poorly welded. This specimen was loaded only in tension and was used primarily to locate the regions of highest stress. No data herein presented.

Before mounting Specimen II in the testing machine it was pressure tested by means of water and air pressure, and all leaks repaired. Data taken during runs with this specimen indicated that the 90 p.s.i. used during the pressure testing had caused permanent set in the specimen. Therefore this specimen, since also obviously too thin, was used to determine the position of highest stresses in the expansion joint with internal pressure. No data or curves for the first two specimens are included in this report.

Specimen III ($t = 0.053 - 0.057$) was first mounted in tensile load only. The specimen was repeatedly elongated from zero to 0.10" for 25 cycles with no internal pressure. Data for this test is recorded in Table 2a, 2b, 2c, 2d. The curves of stress vs. elongation are plotted for the 1st and the 25th cycle in Figures 2 to 12. No data or curves of the intermediate cycles are presented because of the similarity of results of all cycles.

With various constant internal pressures of from 50 - 400 p.s.i. applied, this specimen was then elongated until the strain gages readings indicated the presence of stresses equal to the

highest of those obtained during the 25 cycle test. In these tests the specimen was placed in compression to control the elongation. Finally an attempt was made to vary the elongation with an internal pressure of 600 p.s.i. However, the specimen failed at the weld before 600 p.s.i. was obtained. ($\delta = 0$). The stresses were read from the calibration curve and recorded in Table 3a, 3b, 3c, 3d. Curves are plotted in Figures 13 to 18.

The procedure and treatment of the tests on specimen IV ($t = 0.053 - 0.057$) were the same as those for No. III except that internal pressure was used in all tests. Pressure varied from zero to 500 p.s.i. This specimen withstood the 600 p.s.i. internal pressure for only one half of a cycle (from zero to $0.10''$) before failure at the weld. Data and corresponding curves are shown in Table 4a, 4b, 4c, 4d and Figures 19 to 24.

III

DISCUSSION OF RESULTS

In both the semicircular design discussed in Ref. 4 and the design with the turned up edges studied in this report, stresses beyond the elastic limit of the material were encountered at very small total elongations. In the design with the turned up edges the internal pressure was more critical than it was in the semicircular joint and the amount of deformation increased very appreciably with increasing internal pressure. Curves in Figures 13 to 24 are plots of stress vs. elongation at constant pressures and show the wide variation of stresses encountered as the pressure was increased.

Figs. 2 to 5 show that, with no internal pressure, elongations of 0.045" were obtained with no appreciable permanent set. However, as the pressure was increased, permanent set was noticeable at increasingly smaller elongations. Above 200 p.s.i. stresses beyond the yield were observed even at zero elongation.

In order to evaluate the separate effects of elongation and pressure, the first 0.055" thick specimen (No. III) was run through twenty-five repeated cycles of elongation from zero to 0.10" without any internal pressure. These twenty-five cycles were completed without failure but with a permanent set of 0.020" in total elongation.

Figures 6 to 12 show that after 25 repeated cycles, the stresses encountered during expansion are essentially the same as those found during the initial expansion except for the 0.020" permanent set. The 0.020" permanent set was present after the 1st cycle but remained constant throughout the remainder of the repeated

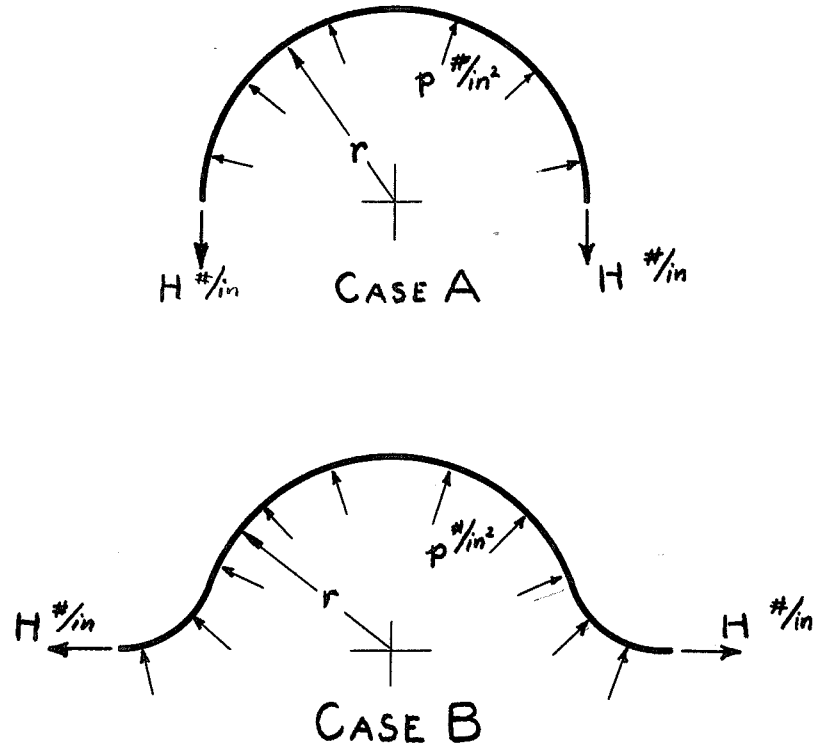
loading test. This indicated that the specimen was capable of many more cycles under the same conditions.

As internal pressure was applied, it was assumed that no failure would occur if the strain gage readings were kept below the readings recorded during the repeated load tests.

On this assumption and a comparison of the curves for specimen III at various internal pressures, the following chart was developed. This chart gives an indication of the maximum total elongation possible for twenty-five cycles at different constant pressures.

<u>P #/in²</u>	<u>δ in.</u>
0	0.10
50	0.10
100	0.080
150	0.074
200	0.070
300	0.050
400	0.020
500	-----
600	0

Failure occurred in this specimen before 600 p.s.i. was reached even at zero deflection. Since the semicircular design was capable of two and one-half cycles from zero to 0.20" with 600 p.s.i., the semicircular expansion joint is more capable of withstanding the high internal pressure. The reason for this is most clearly demonstrated in the accompanying sketch which shows that in Case A membrane stresses in a radial direction are more suitable for withstanding the pressure loads than they are in Case B.



In Case B large membrane stresses in both the circumferential and the axial directions would be required to maintain an equilibrium of forces, since neither of these membrane stresses is capable of contributing much resistance to forces normal to the surface of the expansion joint near the weld. Experimentally, this seemed to be verified since Case A was capable of withstanding 600 p.s.i. in two thicknesses (0.04" and 0.05") while Case B failed before 600 p.s.i. was reached even though the specimen was made of thicker material. ($t = 0.055$ ").

Strain gages mounted at the outermost circumference of the fourth specimen showed that the stresses present at this part of the expansion shell were negative (compression). These stresses remained practically constant as the elongation was varied and the internal pressure was held at given constant values. This

indicates the presence of a bending point of inflection. (See Figures 23 and 24). The combination of the radial contraction of the joint and the apparent bending action results in compressive components in both directions in this region of the joint. In order to better illustrate the stress distribution, both bending and membrane stresses at various points are shown in the accompanying schematic diagram. (See Figure d.)

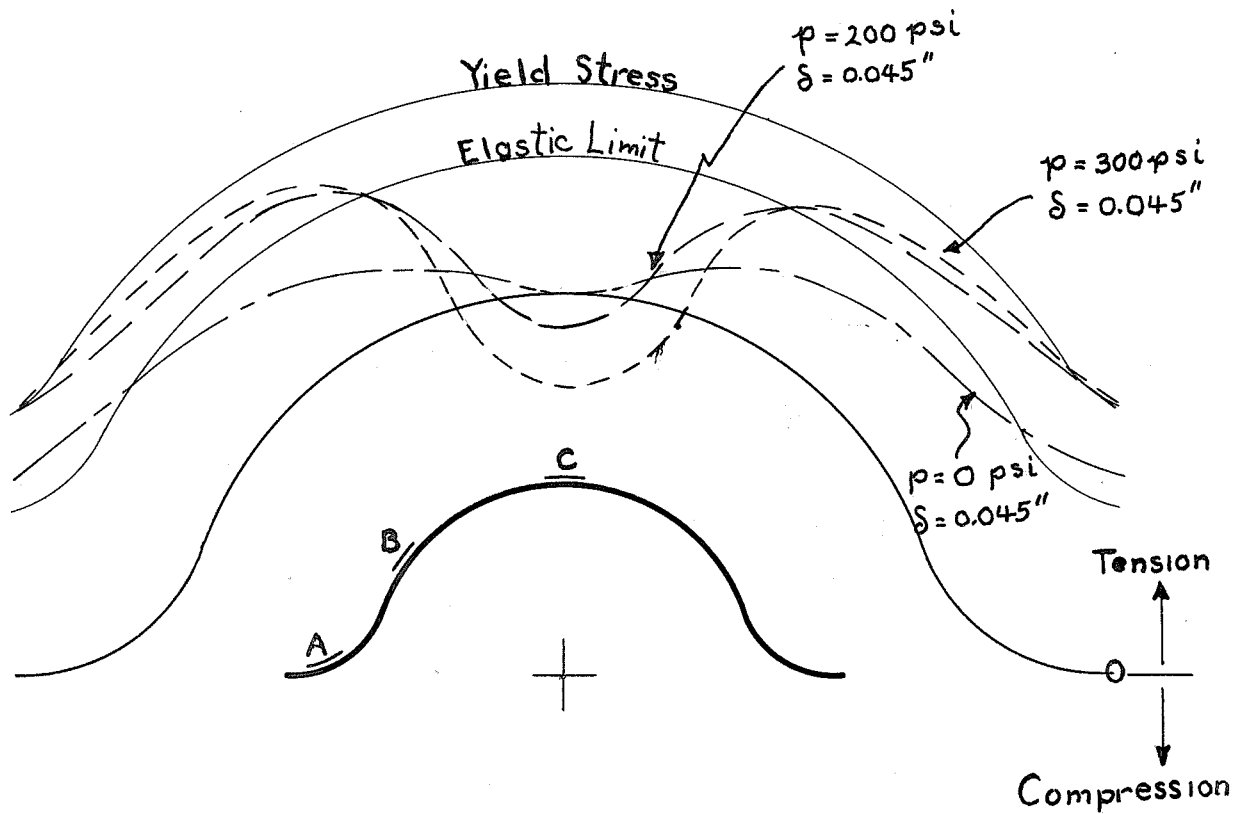
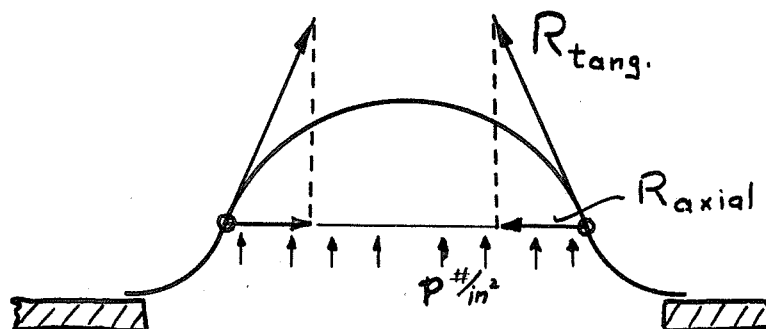


Figure d

An attempt was made to analyse the effect of internal pressure on the spring constant of the expansion joint. However, because the material of the joint exceeded the elastic limit at such small elongations and because the joint changes shape under load the problem is non linear and not easy to discuss. In order to best illustrate the behavior of the spring constant under pressure, curves of the spring constant K are plotted against the elongation of the joint at several internal pressures. (See Fig. 25). The spring constant for these curves was obtained by dividing the difference between the measured axial compressive force and the calculated axial tensile force due to internal pressure by the elongation of the expansion joint.

Over the range of pressures and elongations studied, the spring constant was increased at the small elongations with increases in internal pressure. At elongations close to 0.10", the spring constant at all pressures tended to converge with the spring constant of the expansion ring without internal pressure. This action is probably due to the axial components of the membrane forces that ^{were} developed in the ring by the high internal pressures. (See accompanying figure).

Figure E



On the basis of these tests the expansion joint with the turned up edges was found to be unsatisfactory for the following reasons.

1. The design was incapable of withstanding the design internal pressure of 600 p.s.i.

2. Permanent set was obtained with relatively low internal pressures at elongations of from 0.04 to 0.06".

3. Stresses were the greatest close to the weld where the physical properties of the material were the poorest.

4. The spring constant of the joint increases at high internal pressures.

The design with the turned up edges appeared capable of withstanding greater elongations than the semicircular design as long as the internal pressure was held below 300 p.s.i. Above 300 p.s.i. the semicircular design appeared to be the better of the two.

IV

RECOMMENDATION FOR FUTURE STUDIES

It is believed that a more suitable design is possible by combining the advantages of both of the types studied to date. Fig. f shows a suggested design which should combine these advantages.

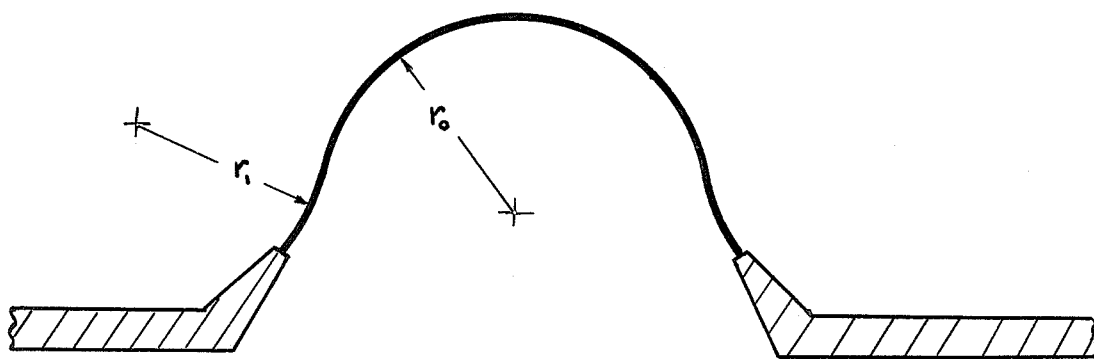


Fig. f

This configuration would make possible the use of the lightest gauge material which would still be capable of withstanding the 600 p.s.i. internal pressure. At the same time it should keep the total force in the axial direction required to elongate the specimen a minimum. This design should also eliminate most of the extreme bending stresses that occurred at the weld of the semi-circular design.

It is further recommended that a more thorough study be made of the effect of the circumferential or hoop stresses on the rigidity of the expansion joint.

V

REFERENCES

1. Theory of Plates and Shells S. Timoshenko
2. Strength of Materials, Vol. II S. Timoshenko
3. Theory of Elasticity S. Timoshenko
4. Some Studies of Expansion Rings in Rocket Motors
Cmdr. N. J. Kleiss, U.S.N.
Lt. Cmdr. S. W. Kerkering,
U.S.N.

VI

INDEX TO TABLES

<u>Page</u>	<u>Table</u>
18	Stress vs. Millivolt Table (steel specimen)
19	Observed gage readings
20	" corrected to Stresses
21	Observed gage readings
22	" corrected to Stresses
23-24	Observed gage readings
25-26	" corrected to Stresses
27-28	Gage readings
29-30	Stresses

VII

INDEX TO FIGURES

<u>Page</u>	<u>Figure</u>
31	a Simplified Drawing of Rocket Motor Showing Temperature Gradient
32	b Test specimen assembly
33	c Strain gage locations
12	d Schematic Diagram of Stresses in Joint
13	e Schematic Diagram of Membrane Forces
15	f Proposed Design

VII

INDEX TO PHOTOS

34	I. General View of Test
35	II. General View of Mounted Specimen
36	III. General View of Specimen

TABLE 1
Stress-Millivolt Curve

Area = 0.061 x 0.50 = 0.0305 sq. in.

Load	Gage 1	Gage 2	Gage 3	Δv 1	Δv 2	Δv 3	Ave.	Stress σ
50	.063	.268	.256	.063	.268	.256	.196	1640
100	.250	.379	.387	.187	.111	.131	.339	3280
150	.420	.488	.508	.170	.109	.121	.472	4920
200	.615	.615	.631	.195	.127	.123	.620	6560
250	.791	.740	.753	.176	.125	.122	.762	8200
300	.960	.861	.879	.169	.121	.126	.900	9840
350	1.097	.992	.995	.137	.131	.116	1.060	11480
400	1.266	1.097	1.100	.105	.105	.169	1.155	13120
450	1.432	1.237	1.237	.144	.140	.137	1.302	14760
500	1.592	1.372	1.359	.160	.135	.122	1.441	16400
550	1.753	1.510	1.487	.161	.138	.128	1.583	18010
600	1.912	1.648	1.615	.159	.138	.128	1.725	19680
650	2.077	1.783	1.739	.165	.135	.124	1.866	21310
700	2.233	1.930	1.873	.156	.147	.134	2.012	22950
750	2.390	2.070	2.005	.157	.140	.132	2.155	24600
800	2.550	2.213	2.130	.160	.143	.125	2.298	26210
850	2.708	2.359	2.266	.158	.146	.136	2.444	27900
900	2.863	2.506	2.392	.155	.147	.124	2.587	29500
950	3.014	2.653	2.520	.151	.147	.128	2.729	31900
1000	3.171	2.797	2.653	.157	.144	.133	2.874	32800
1050	3.322	2.949	2.787	.151	.152	.134	3.019	34500
1100	3.470	3.090	2.918	.148	.141	.131	3.159	36100
1150	3.618	3.238	3.049	.148	.148	.131	3.302	37700
890	5.015			1.397			5.015	29200
908	10.423	Gages went		5.480			10.423	29800
933	11.080	bad.		.653			11.080	30600
1000	11.715			.635			11.715	32800
1034	12.710			.995			12.710	33930
1036	13.163			.453			13.163	33950

All Gage readings are in Millivolts
and all Stresses are in lbs/sq. in.

TABLE 2a

Specimen III

t = 0.055" No Internal Pressure
1st Cycle Tension Only

Load lbs.	δ " $\times 10^{-3}$	Gage						
		1	2	3	4	5	7	6
74748	5	.193	.250	.378	.307	.083	.037	.175
1947	10	.657	.885	.981	1.912	.400	.241	.563
3068	15	.969	1.347	1.464	1.408	.562	.413	.871
4327	20	1.367	1.886	1.967	1.908	.750	.512	1.192
5293	25	1.582	2.197	2.323	2.278	.871	.545	1.386
6241	30	1.879	2.625	2.751	2.622	1.035	.631	1.664
7227	35	2.110	2.945	3.092	3.011	1.198	.728	1.910
8265	40	2.419	3.369	3.522	3.391	1.357	.806	2.177
9330	45	2.708	3.757	3.929	3.814	1.510	.933	2.484
10272	50	3.013	4.142	4.284	4.165	1.648	.989	2.694
11382	55	3.265	4.527	4.708	4.591	1.813	1.063	3.010
12305	60	3.539	4.956	5.052	4.939	1.957	1.148	3.200
13417	65	3.800	5.392	5.497	5.345	2.137	1.241	3.549
14352	70	4.060	5.838	5.878	5.644	2.259	1.307	3.771
15320	75	4.277	6.252	6.223	5.975	2.452	1.394	4.078
16265	80	4.560	6.671	6.544	6.259	2.572	1.490	4.311
16925	85	4.758	7.041	6.904	6.497	2.740	1.625	4.588
17565	90	5.050	7.411	7.203	6.720	2.901	1.802	4.818
18025	95	5.318	7.657	7.359	6.849	3.105	2.068	5.088
18400	100	5.436	8.003	7.552	7.011	3.333	2.335	5.282

TABLE 2b
Specimen III

Load lbs.	$\times 10^{-3}$ δ''	Stresses psi						
		Gage 1	2	3	4	5	7	6
748	5	1800	2800	4200	3250	800	200	1750
1947	10	7300	9950	11100	10200	4450	2600	6200
3068	15	10900	15150	16400	15900	6200	4600	9800
4327	20	15350	21350	22250	21500	8400	5700	13400
5293	25	17800	24800	26200	25800	9800	6000	15800
6241	30	21300	29700	31100	29600	11500	7100	18700
7227	35	23800	36200	35000	33900	13400	8100	21600
8265	40	27250	38000	38350	38200	15250	8500	24500
9330	45	30600	38100	36900	37750	17000	10400	28100
10272	50	34000	35100	34000	35000	18500	11100	30400
11382	55	36975	32300	31100	31850	20450	11800	34000
12305	60	38290	29900	29400	29900	22200	12800	36200
13417	65	37800	28050	27750	28250	24000	14000	38350
14352	70	36000	26850	26700	27300	25500	14700	37950
15320	75	34200	25950	25950	26450	27700	15750	35800
16265	80	32100	25400	25600	25950	29000	16800	33750
16925	85	30900	25300	25350	25600	31000	18300	31900
17565	90	29400	25350	25250	25400	32800	20300	30550
18025	95	28350	25400	25300	25350	35100	23400	29300
18400	100	27975	25550	25350	25300	37700	26350	28500

TABLE 2c

Specimen III

t = 0.055"
25th Cycle

No Internal Pressure
Tension Only

Load lbs.	x 10 ⁻³ S"	Gage Millivolts							
		1	2	3	4	5	7	6	
0	26	-.180	.880	.180	-.480	.490	.802	.424	
3260	40	.835	2.340	1.590	.896	1.070	1.150	1.540	
7345	60	2.240	4.160	3.360	2.600	1.770	1.535	2.710	
11875	80	3.620	6.010	5.160	4.410	2.490	1.952	4.014	
16235	100	5.075	7.904	6.922	6.145	3.140	2.302	5.100	

TABLE 2d

Load lbs.	$\times 10^{-3}$ S''	Gage		Stresses					
		1	2	3	4	5	7	6	
0	26	-1800	9900	1800	-5200	5300	9000	4600	
3260	40	9300	26400	18000	10000	115800	13000	17400	
7345	60	25300	35100	37900	29400	19900	17200	30600	
11875	80	38300	26400	29000	33100	28200	22100	36400	
16235	100	29300	25500	25300	26100	35500	26000	29200	

TABLE 3a

Specimen III

t = 0.055

With Internal Pressure

Load (lbs.)	p p.s.i.	δ " $\times 10^{-3}$	Gage Millivolts						
			1	2	3	4	5	6	7
10,730	50	24	-1.082	-.292	-.800	-1.335	.530	.067	.122
7,370		34	-.060	1.047	.491	-.158	1.043	.962	.222
4,100		44	1.044	2.437	1.857	1.070	1.600	1.939	.292
14,350	100	24	-.738	.180	-.248	-.813	1.030	.712	N.G.
11,580		34	.288	1.472	1.028	.361	1.545	1.602	
9,170		44	1.498	3.133	2.604	1.827	2.217	2.732	
5,000		54	2.482	4.420	3.818	2.956	2.642	3.540	
1,900		64	3.794	6.150	5.430	4.395	3.260	4.630	
20,125	150	24	-.228	.950	.470	-.203	1.665	1.577	
16,925		34	.918	2.477	1.940	1.190	2.227	2.583	
14,040		44	2.000	3.928	3.325	2.500	2.773	3.542	
10,525		54	3.100	5.380	4.705	3.802	3.265	4.453	
7,285		64	4.068	6.780	6.015	5.000	3.700	5.335	
4,350		74	4.932	8.240	7.353	6.042	3.867	6.218	
25,575	200	24	-.010	1.708	1.100	.120	1.910	2.495	
22,210		34	1.188	3.313	2.465	1.578	2.490	3.532	
18,600		44	2.322	4.820	4.070	2.957	3.022	4.463	
15,320		54	3.393	6.233	5.417	4.260	3.533	5.400	
17,305		64	4.363	7.645	6.718	5.490	3.751	6.518	
9,965		74	5.190	9.793	8.265	6.718	3.821	7.610	

TABLE 3b

Load lbs	p p.s.i.	$\times 10^{-3}$ S"	Gage Millivolts					
			1	2	3	4	5	6
36,880	300	24	.681	3.947	2.755	1.250	2.845	5.034
33,840		34	1.120	4.968	3.662	1.880	4.733	7.846
32,200		44	2.451	6.626	5.240	3.455	5.245	8.830
27,000		54	4.138	8.712	7.320	5.525	5.210	9.561
25,000		64	6.170	11.705	10.242	8.200	4.430	9.540
23,320		74	8.700	15.850	14.342	11.980	3.760	9.610
52,200	400	24	3.690	9.546	8.374	6.030	3.377	7.534
48,425		34	5.170	11.228	9.907	7.614	4.434	9.250
44,750		44	6.650	12.690	11.325	9.035	4.757	10.290
42,075		54	7.680	14.680	13.570	11.076	4.764	11.260
40,405		64	10.038	18.280	17.730	14.842	4.513	12.123
38,580		74	13.253	N.G.	N.G.	19.200	4.414	12.572

TABLE 3c

Stresses

Load lbs.	p psi	$\times 10^{-3}$ S''	1	2	3	4	5	6
10730	50	24	-12200	-3200	-9000	-15000	5900	500
7370	50	34	- 400	11600	5400	- 1700	11600	10800
4100	50	44	11600	27500	21200	12100	18000	21900
14350	100	24	- 8200	1800	-2700	- 9100	11500	8000
11580	100	34	3200	16600	11400	4000	17400	18000
9170	100	44	16900	35400	29400	20500	25000	31000
5000	100	54	28100	33000	37800	33500	29800	38300
1900	100	64	337900	26100	28000	33200	37000	31700
20125	150	24	-22500	10700	5200	- 2100	18600	17700
16925	150	34	10200	28100	22000	13300	25200	29200
14040	150	44	22700	37000	37700	28300	31400	38300
10525	150	54	35100	28100	31100	37800	37100	32800
7285	150	64	36000	25400	26400	29700	38200	28300
4350	150	74	30000	24800	25300	26300	37400	26000
25575	200	24	--	19200	12400	1100	21600	28100
22210	200	34	13300	37400	27800	12200	28100	38300
18600	200	44	26200	30700	35900	33600	34100	32700
15320	200	54	38200	26000	28000	34200	38300	28100
12305	200	64	33400	25400	25400	27700	38000	25600
9965	200	74	28800	27800	25800	25400	37700	25300
36880	300	24	7600	36800	31200	14000	32100	29600
33840	300	34	12500	29900	38200	21300	30900	25500
30220	300	44	27500	25500	28600	38300	38600	26400
27000	300	54	35200	26200	25300	27600	28700	27500
25000	300	64	26100	31800	28600	25700	33000	27400
23320	200	74	26100	39400	36800	32300	38000	27600

TABLE 3d

Stresses

Load lbs.	p psi.	$\times 10^{-3}$ S''	1	2	3	4	5	6
52200	400	24	38200	26700	25900	26400	38000	25300
48425	400	34	28800	30700	28000	25300	32900	27000
44750	400	44	25400	33700	30900	26600	30900	28800
42075	400	54	25400	37400	35400	30300	30800	30800
40405	400	64	28200	43700	42100	37700	32500	32600
38580	400	74	34800			44500	35300	33400

TABLE 4a

Specimen IV

t = 0.055

With Internal Pressure

Load lbs.	psi P	$\times 10^{-3}$ S"	Gage Millivolts									
			1	2	3	4	6	7	8	9	10	
8270	50	0	.278	.455	.550	.412	.885	1.072	.622	-.328	-.170	
66355		10	1.374	1.540	1.603	1.513	1.281	1.860	.965	-.392	-.040	
4150		20	2.142	2.412	2.496	2.417	1.568	2.502	1.186	-.415	+.080	
2500		30	2.923	3.277	3.360	3.324	1.824	3.115	1.422	-.455	+.200	
1650		35	3.420	3.852	3.988	4.096	1.773	3.390	1.508	-.462	+.270	
13000	100	0	1.575	1.070	1.518	1.510	1.000	1.273	.850	-.512	-.260	
11800		10	2.146	2.082	2.400	2.429	1.448	2.210	1.231	-.575	-.130	
8675		20	2.735	2.983	3.200	3.259	1.742	2.933	1.465	-.581	+.030	
6500		30	3.313	3.905	3.817	4.088	2.067	3.702	1.741	-.604	+.150	
5270		40	3.792	4.700	4.828	4.935	2.093	4.361	1.960	-.653	+.270	
3650		50	4.118	5.377	5.482	5.746	2.130	4.800	2.073	-.662	+.400	
2715		60	4.320	6.077	6.073	6.642	2.322	5.250	2.220	-.679	+.550	
1500		70	4.508	6.700	6.558	7.431	2.688	5.363	2.245	-.687	+.720	

TABLE 4b

Specimen IV

Load lbs.	psi P	$\times 10^{-5}$ S"	Gage Millivolts									
			1	2	3	4	6	7	8	9	10	
25,100	200	10	1.448	2.390	2.797	3.440	1.055	2.753	1.752	- 1.060	- .432	
23,400		20	2.075	3.400	3.698	4.353	1.457	3.547	2.045	- 1.122	- .310	
20,625		30	2.682	4.337	4.530	5.219	1.720	4.239	2.290	- 1.145	- .163	
19,180		40	3.137	5.080	5.177	5.950	1.942	5.024	2.481	- 1.210	- .058	
17,670		50	3.572	5.832	5.962	6.640	1.937	5.618	2.470	- 1.280	.000	
16,200		60	4.110	6.600	6.917	7.440	1.720	6.135	2.328	- 1.450	+ .015	
15,750		70	4.672	7.500	7.988	8.480	1.413	6.362	2.045	- 1.565	+ .070	
41,000	300	10	.842	2.292	2.950	3.452	.381	2.756	1.218	- 1.920	-1.170	
38,670		20	1.468	3.462	3.970	4.572	.917	3.631	1.612	- 2.010	-1.046	
35,170		30	2.155	4.475	4.988	5.591	1.328	4.508	1.920	- 2.050	- .892	
32,950		40	2.768	5.457	5.868	6.495	1.830	5.527	2.228	- 2.150	- .832	
31,600		50	3.175	6.141	6.661	7.233	1.946	6.142	2.254	- 2.270	- .812	
30,850		60	3.812	7.233	7.730	8.188	2.013	6.940	1.955	- 2.578	- .945	
67,500	500	10	-2.928	3.238	2.724	3.090	7.725	7.727	6.020	- 8.327	-7.012	
64,500		20	-2.225	4.963	4.249	4.940	8.757	8.736	5.970	- 9.308	-7.330	
63,875		30	-1.639	6.917	5.622	6.912	9.220	8.500	5.902	-10.383	-7.910	
62,760		40	- .850	9.296	7.449	9.420	9.400	7.250	5.579	-11.260	-8.221	
60,500		50	+ .294	12.200	9.762	12.217	9.632	5.457	5.326	-12.348	-8.698	
58,135		60	1.500			15.283	9.345	4.727	4.850	-12.819	-8.725	
56,200		70	3.398			19.250	9.000	3.639	4.310	-13.215	-8.773	
55,305		80	5.360				8.728	2.255	3.810	-13.752	-8.812	
53,870		90	8.540				8.378	1.500	3.333	-14.072	-8.770	
52,000		100					7.995	.903	2.896	-14.257	-8.609	

TABLE 4c

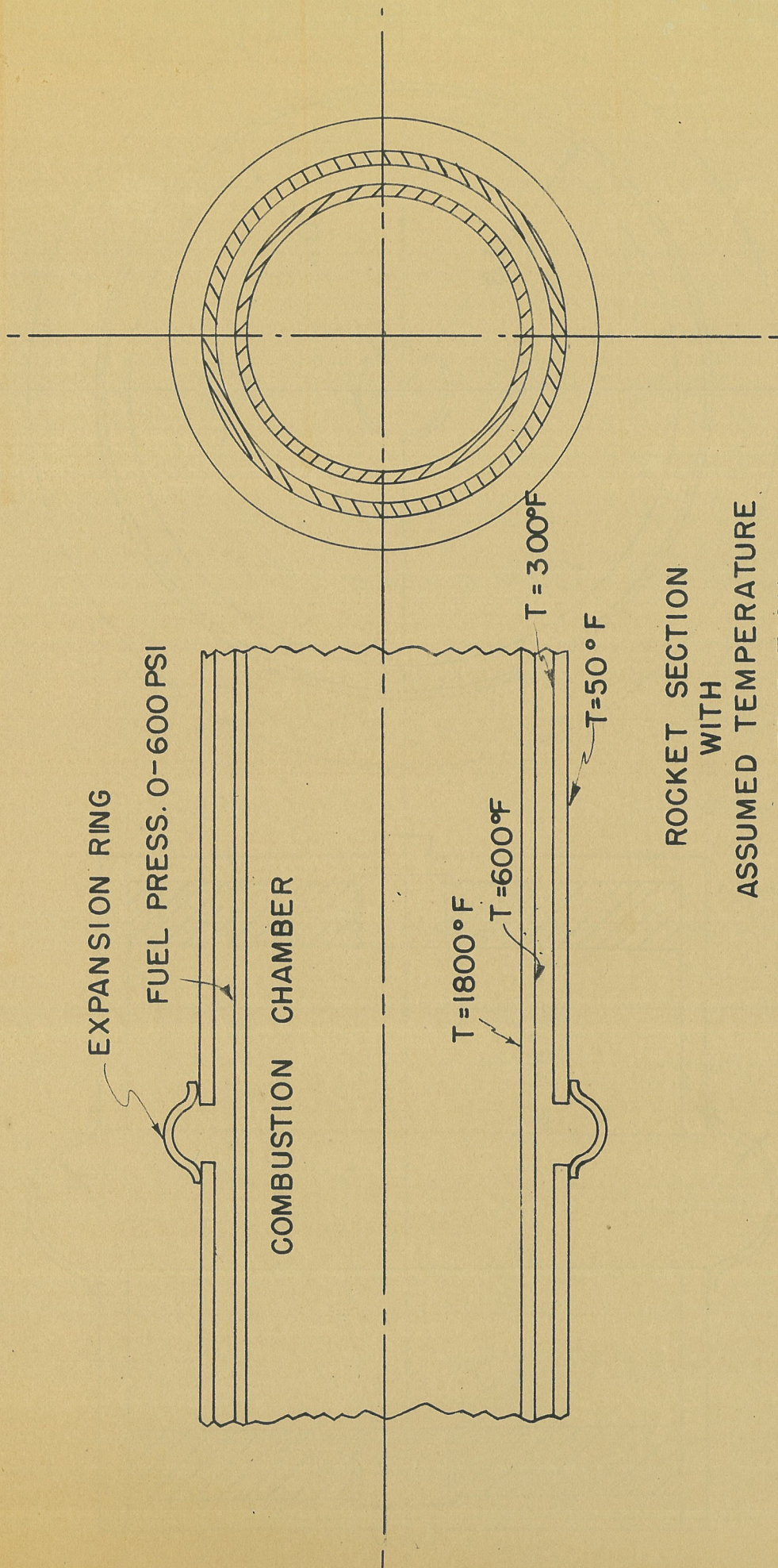
Specimen IV

Load lbs.	P psi	$\times 10^{-3}$ S''	Stresses									
			1	2	3	4	6	7	8	9	10	
8270	50	0	3000	5000	6100	4600	9900	12100	7000	-3500	-1800	
6355		10	15500	17400	18000	17000	14400	21000	10800	-4200	-200	
4150		20	24200	27300	28200	27300	17700	28200	13200	-4500	700	
2500		30	33000	37100	38100	37600	20400	35200	16000	-5000	2100	
1650		35	38200	37600	36500	35700	19900	38200	17000	-5200	3000	
13000	100	0	17800	12100	17100	17000	11200	14100	9500	-5700	-2800	
11800		10	24000	23500	27200	27500	16300	25000	13800	-6400	-1300	
8675		20	30800	33900	36200	37000	19600	33100	16400	-6500	100	
6500		30	37400	37100	37800	35700	23300	38200	19700	-6600	1600	
5270		40	37800	31200	30500	30000	23600	33400	22200	-7100	3000	
3650		50	35500	28100	27800	27000	24100	30600	23500	-7200	4400	
2715		60	33800	26200	26300	25500	26100	28600	25000	-7500	6100	
1500		70	32400	25400	25600	25300	30300	28200	25300	-7600	8000	

TABLE 4d

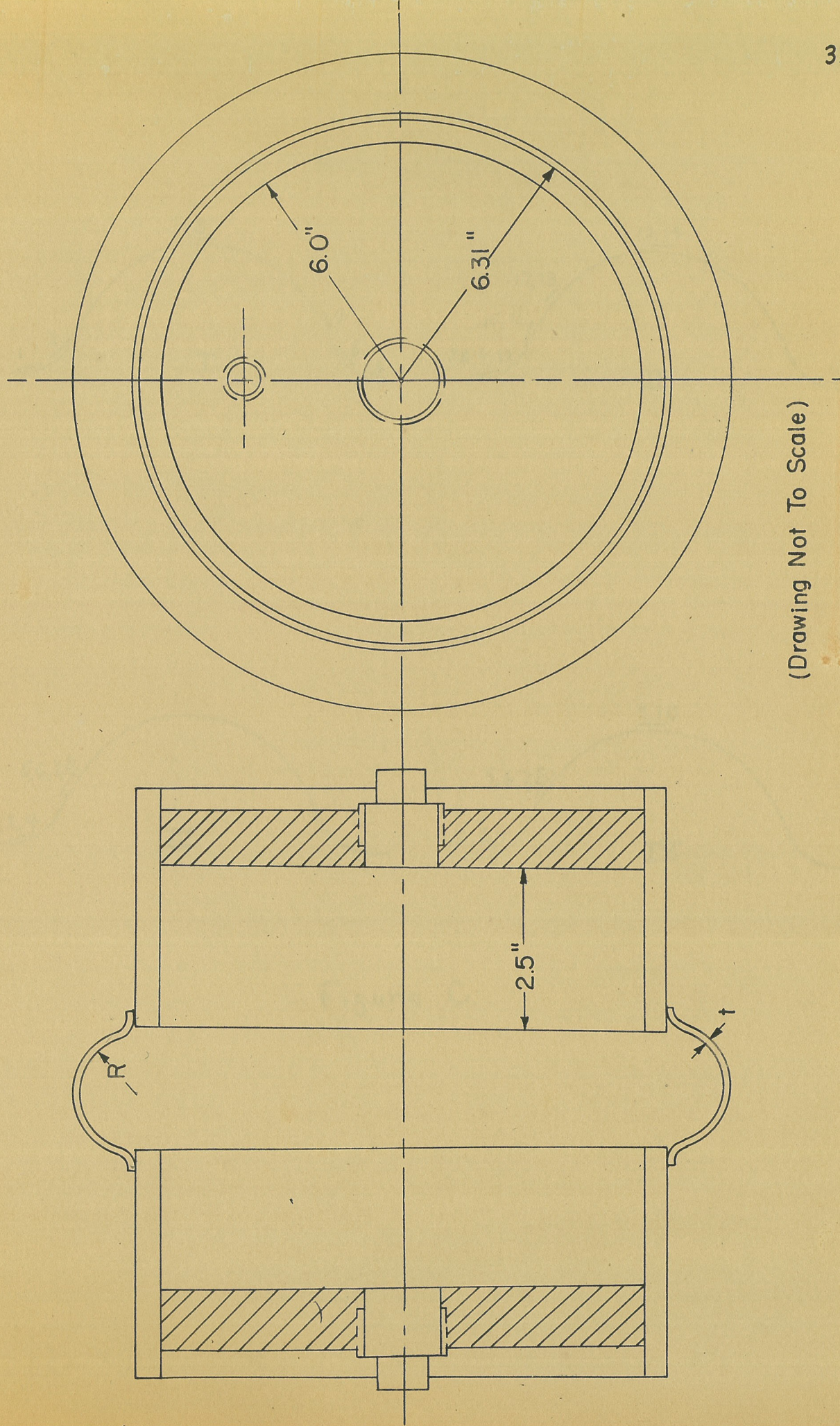
Specimen IV

Load lbs.	p p.s.i.	$\delta \times 10^{-3}$ δ"	Stresses									
			1	2	3	4	6	7	8	9	10	
25100	200	10	16400	27100	31600	38300	11600	31200	19800	-11900	-4700	
23400		20	23400	38200	38200	33400	16400	38300	23000	-12600	-3400	
20625		30	30300	33600	32400	28700	19500	34400	26000	-12900	-1600	
19180		40	35400	29400	28900	26500	22000	29600	28100	-13400	-100	
17670		50	38300	26800	26500	25500	21900	27400	28000	-14400	0	
16200		60	35500	25500	25300	25300	19500	26200	26200	-16500	100	
15750		70	31400	25300	25600	26000	15900	25800	23000	-17700	200	
41000	300	10	9400	25900	33400	38300	4200	31200	13700	-21600	-13200	
38670		20	16500	38300	36700	32000	10200	38300	18100	-22700	-11500	
35170		30	24500	32600	29700	27400	14900	32500	21600	-23200	-9900	
32950		40	31200	27900	26700	25600	20600	27700	25200	-24300	-9400	
31600		50	35900	26200	25500	25300	22100	26100	25600	-25600	-9200	
30850		60	37800	25300	25400	25700	22800	25300	22200	-29200	-10700	
67500	500	10	-33000	36500	30800	35000	25400	25400	26400	-25900	-25300	
64500		20	-25200	29800	34300	29900	26300	26200	26500	-27000	-25300	
63875		30	-18400	25300	27400	25300	26900	26000	26600	-28900	-25500	
62760		40	-9500	27000	25300	27200	27200	25300	27500	-30800	-25700	
60500		50	3200	32700	22800	32700	27600	27900	28400	-33000	-26200	
58135		60	11200			38400	27100	31000	30400	-33900	-26250	
56200		70	38200			44500	26600	38300	33900	-34700	-26300	
55305		80	28200				26200	25600	37800	-35700	-26400	
53870		90	26000				25900	16900	37200	-36300	-26300	
52000		100					25500	10200	32700	-36600	-26100	



ROCKET SECTION
WITH
ASSUMED TEMPERATURE
DISTRIBUTION

FIG. a



(Drawing Not To Scale)

FIG. b

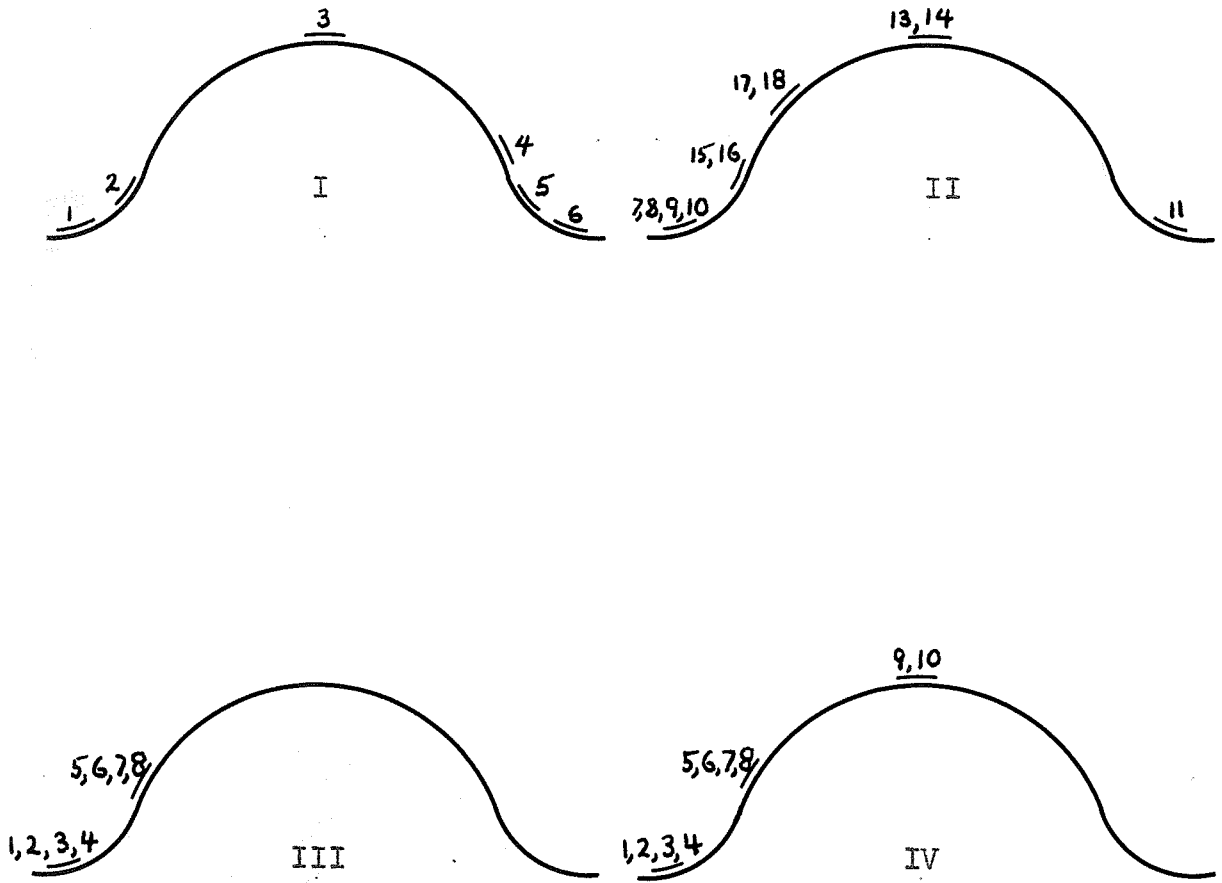
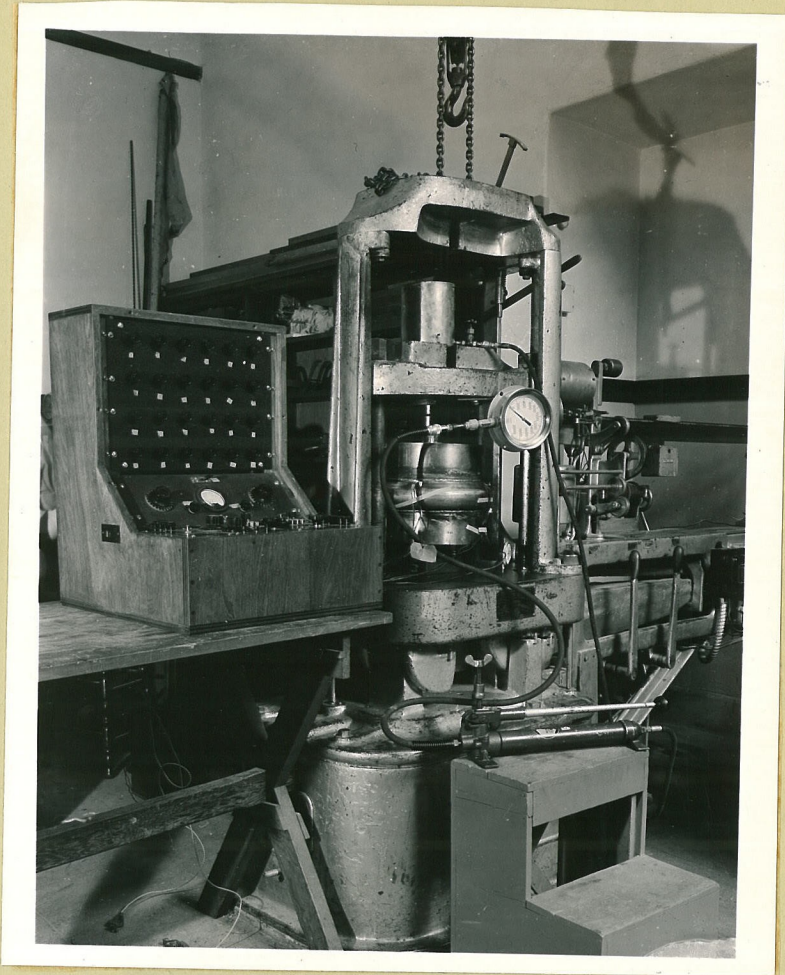
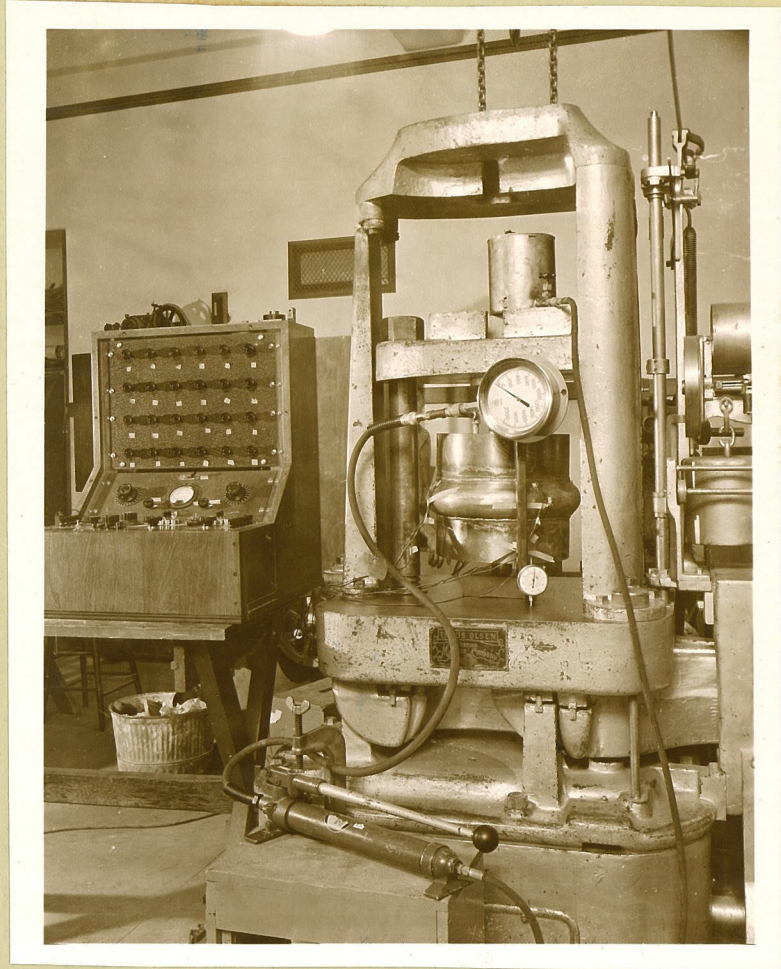


Figure C.



Photograph I



Photograph II



Photograph III

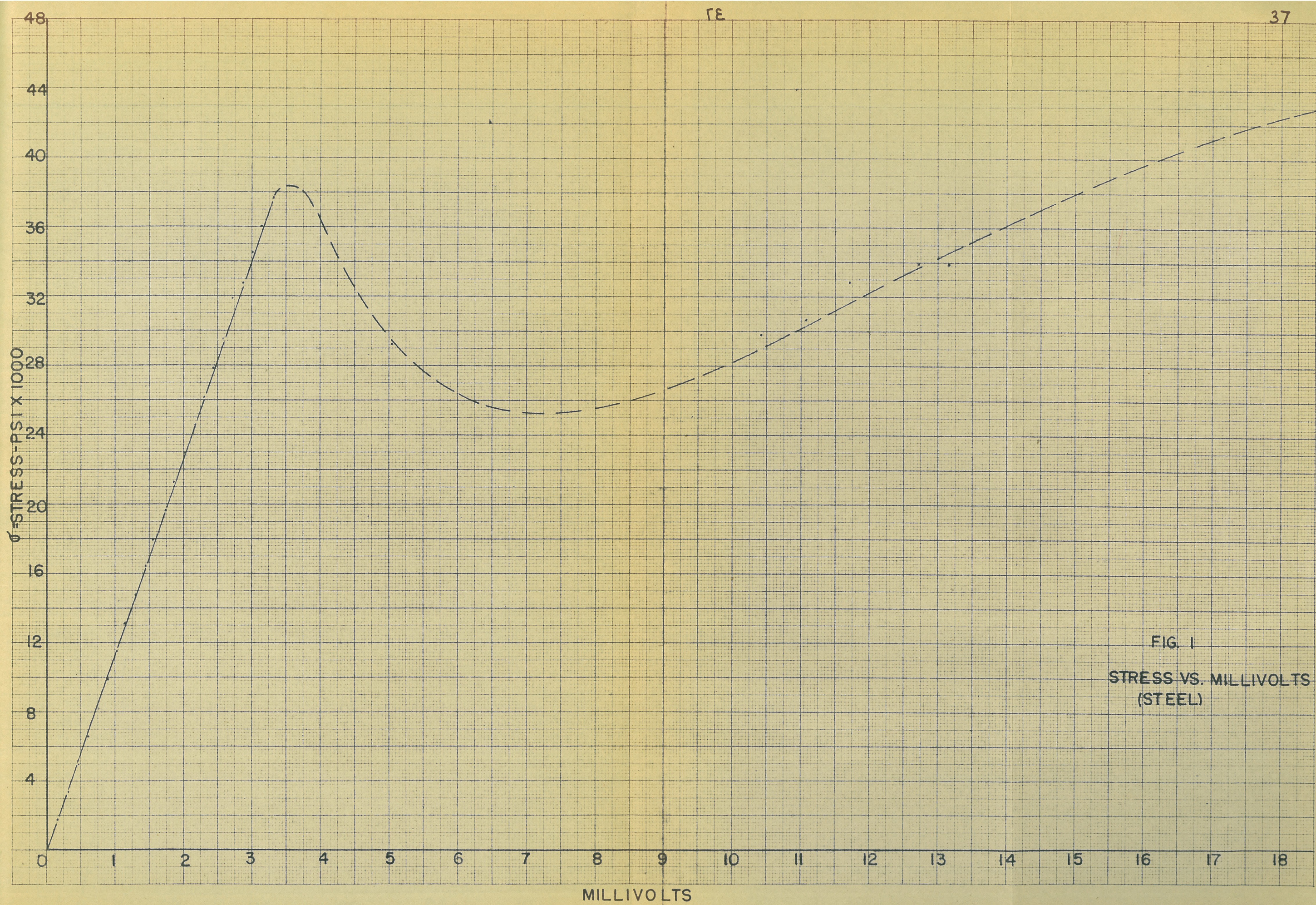


FIG. 1
STRESS VS. MILLIVOLTS
(STEEL)

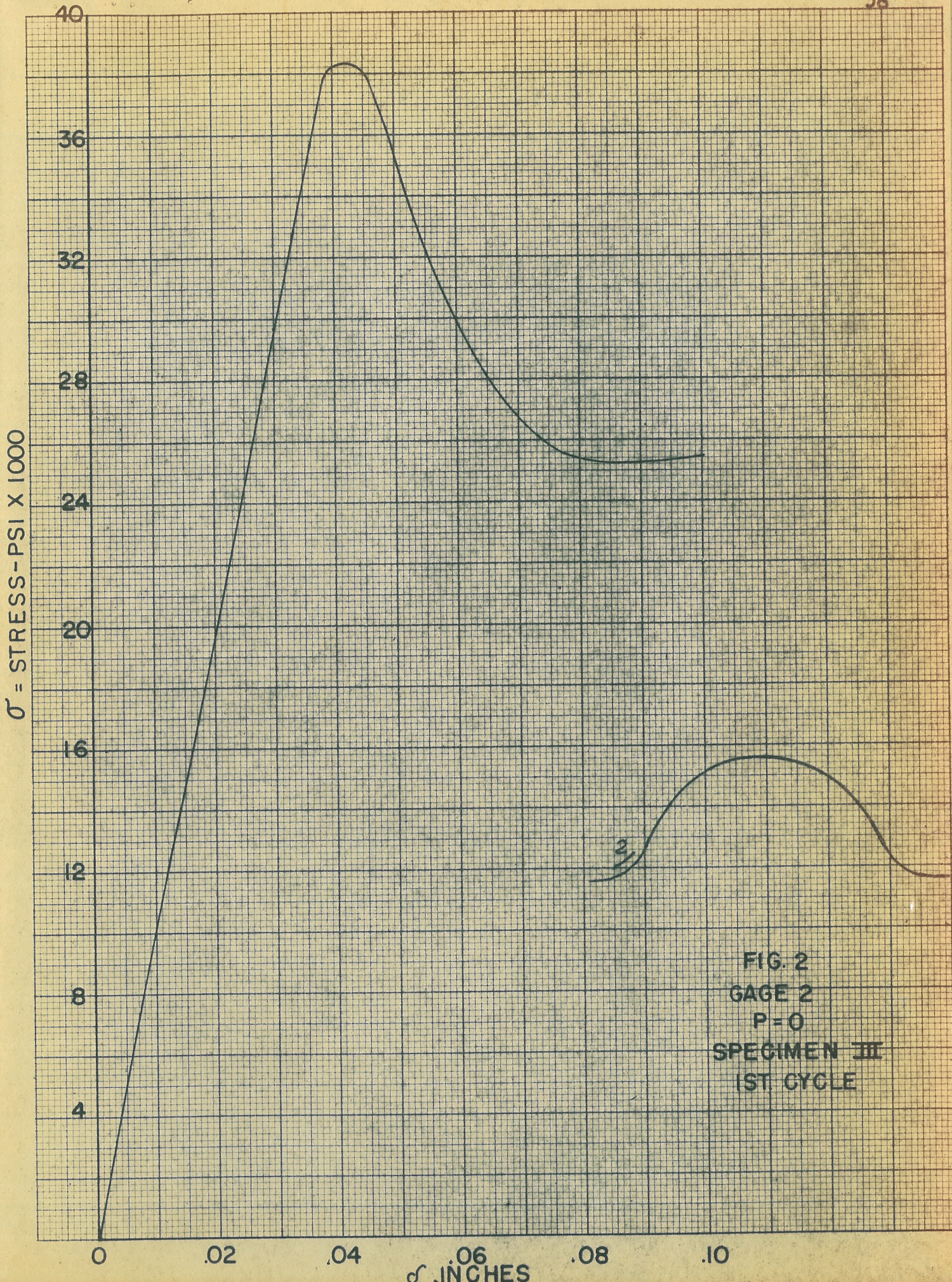
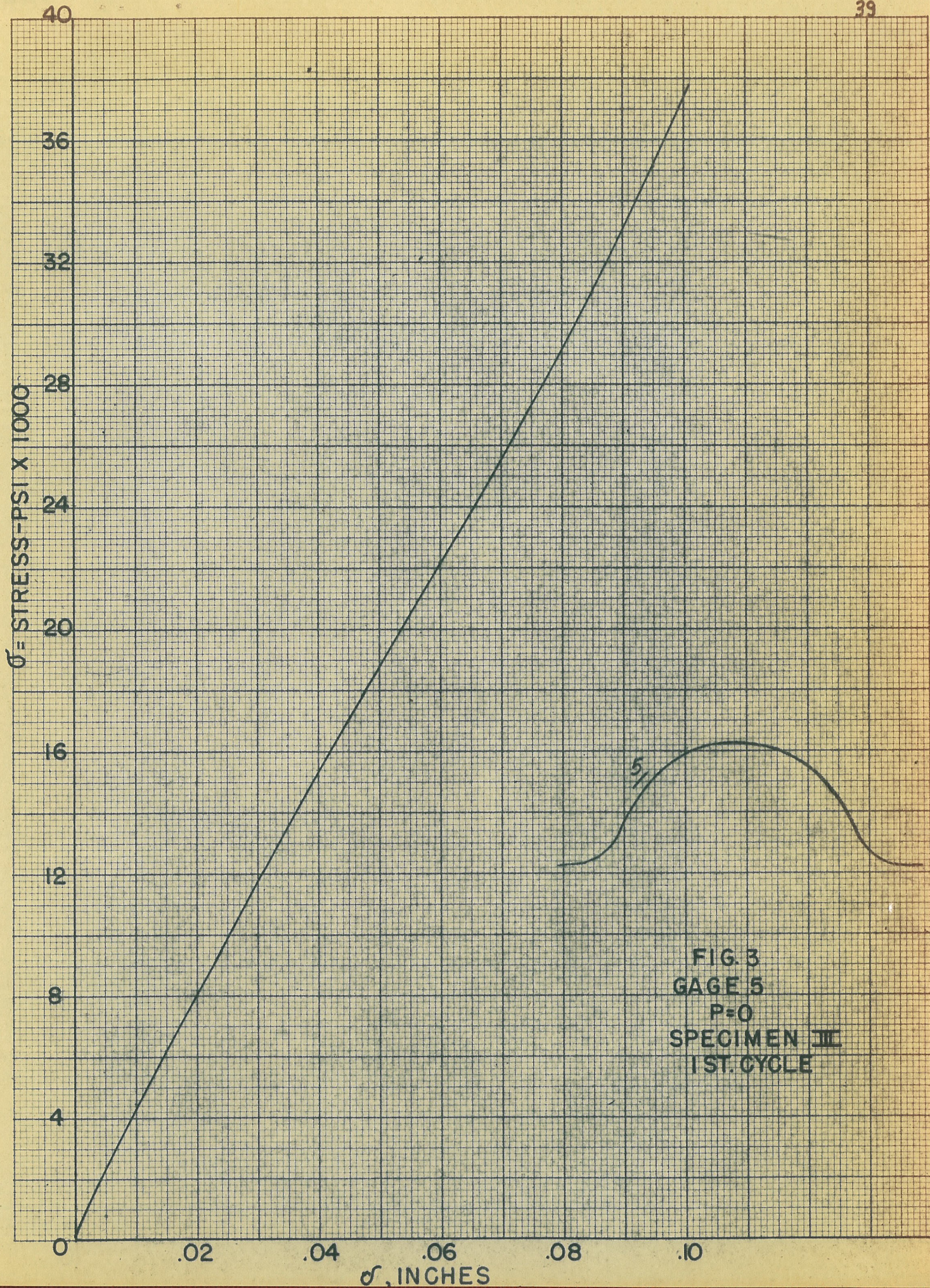


FIG. 2
GAGE 2
P=0
SPECIMEN III
1ST. CYCLE



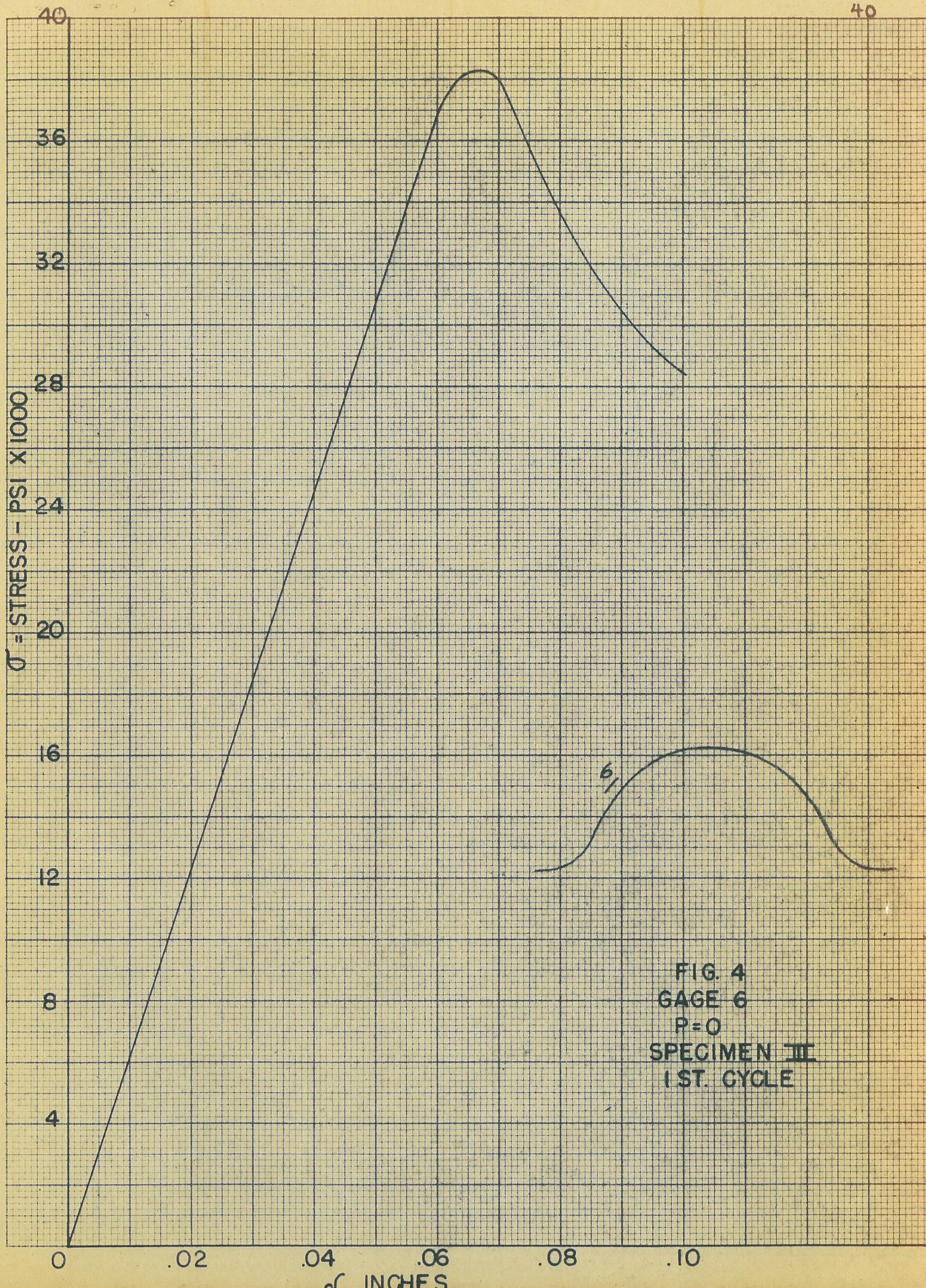


FIG. 4
GAGE 6
P=0
SPECIMEN III
1ST. CYCLE

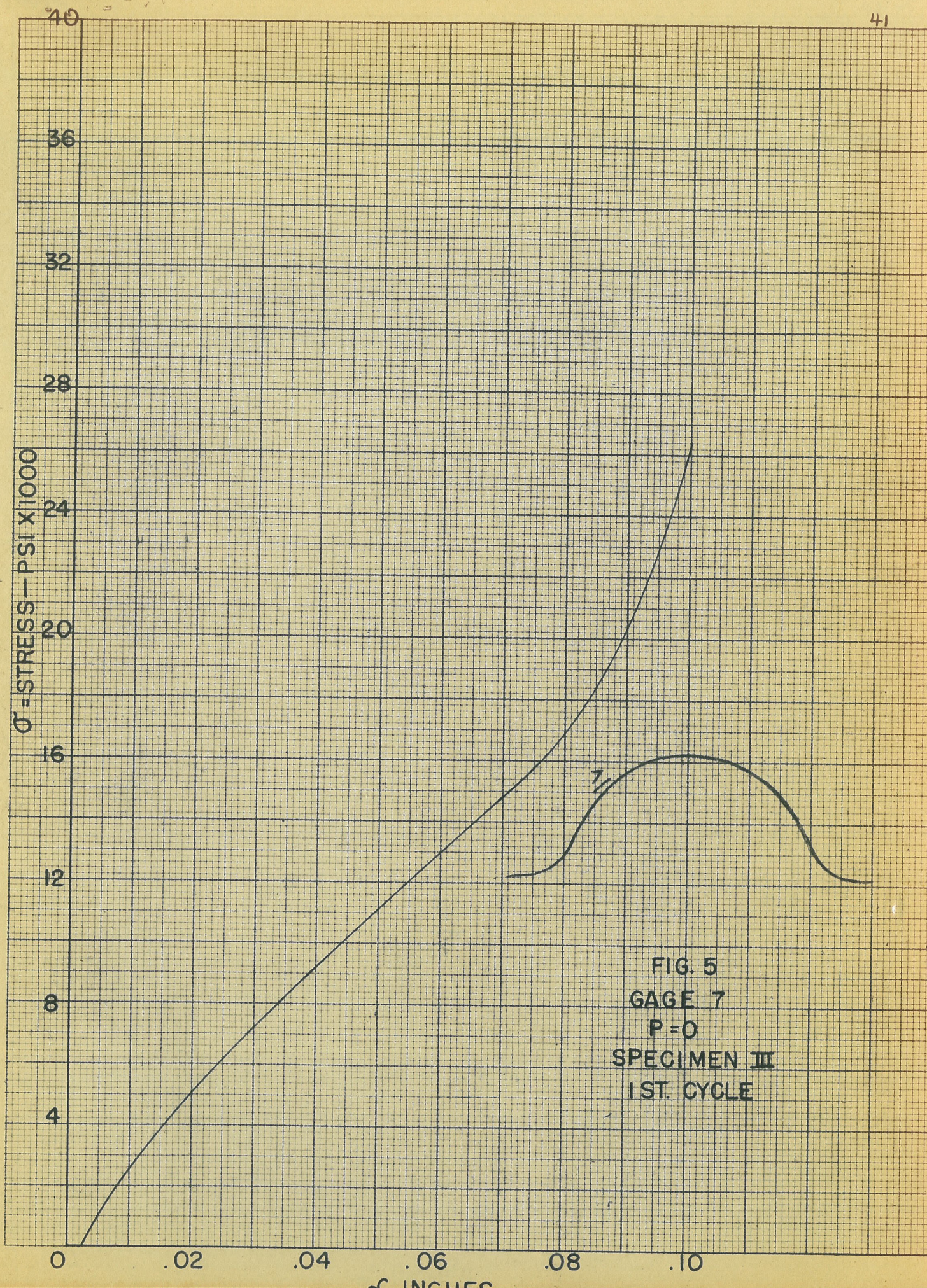


FIG. 5
GAGE 7
P=0
SPECIMEN III
1ST. CYCLE

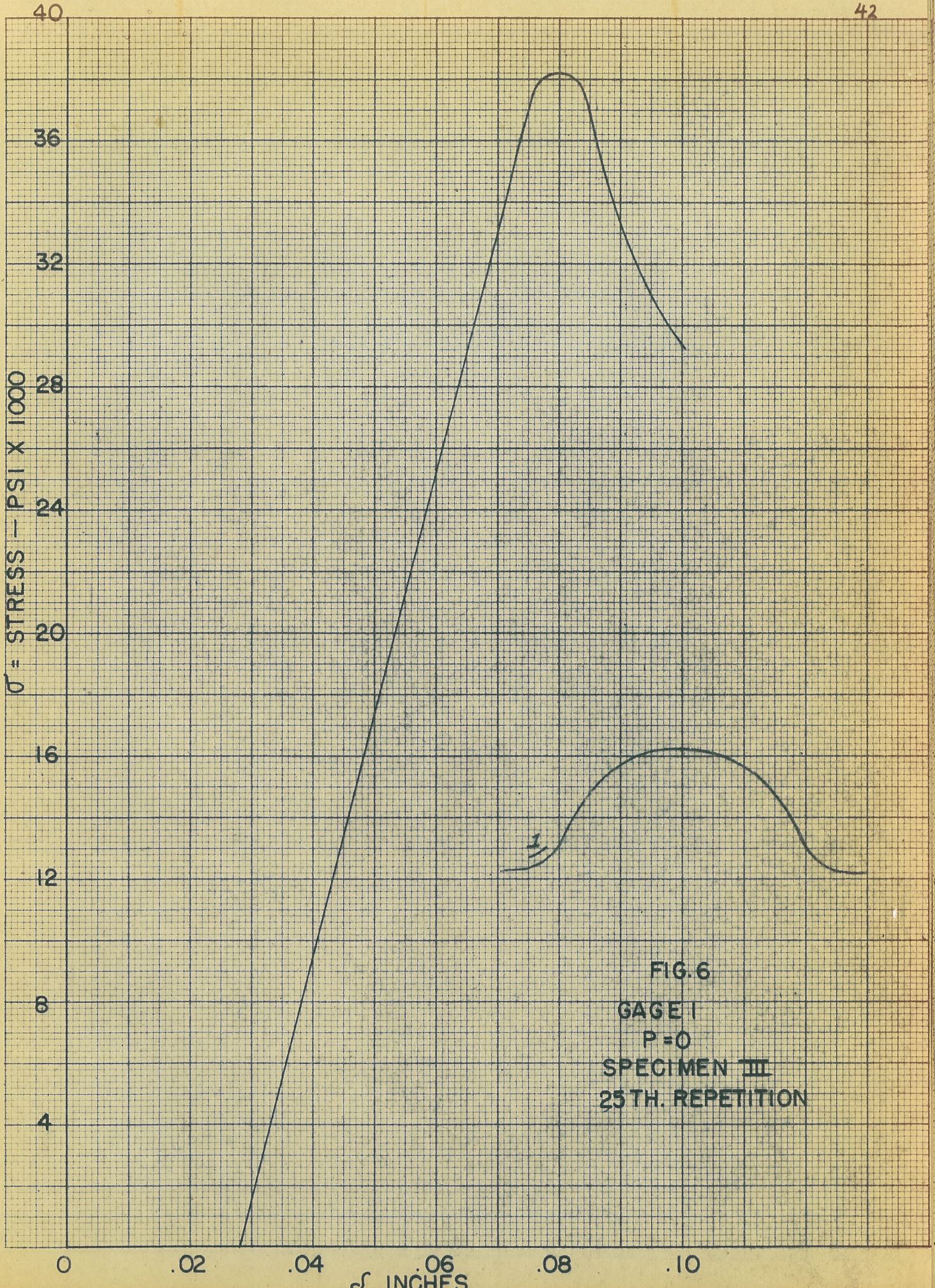
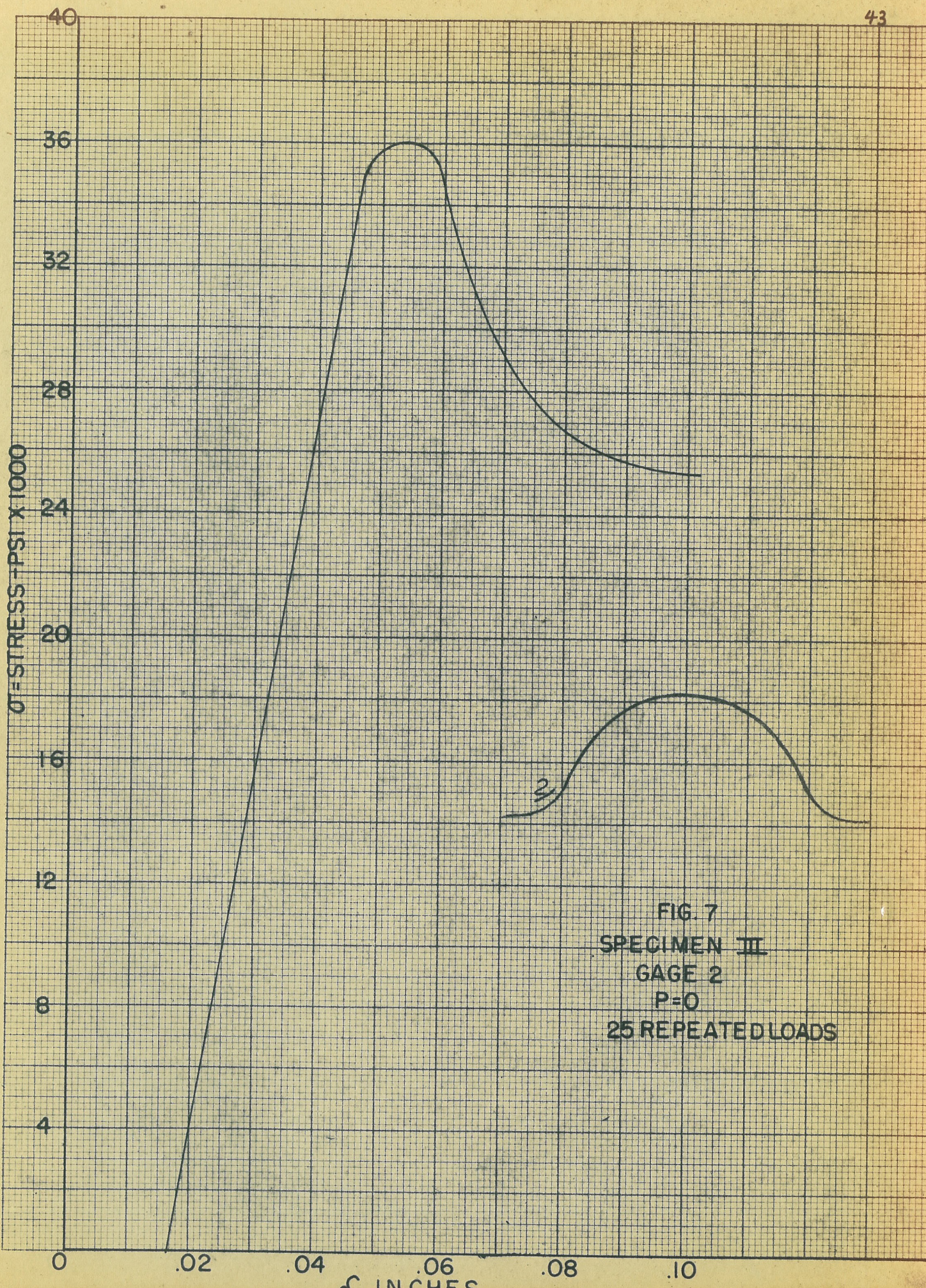


FIG. 6
GAGE I
P=0
SPECIMEN III
25TH. REPETITION



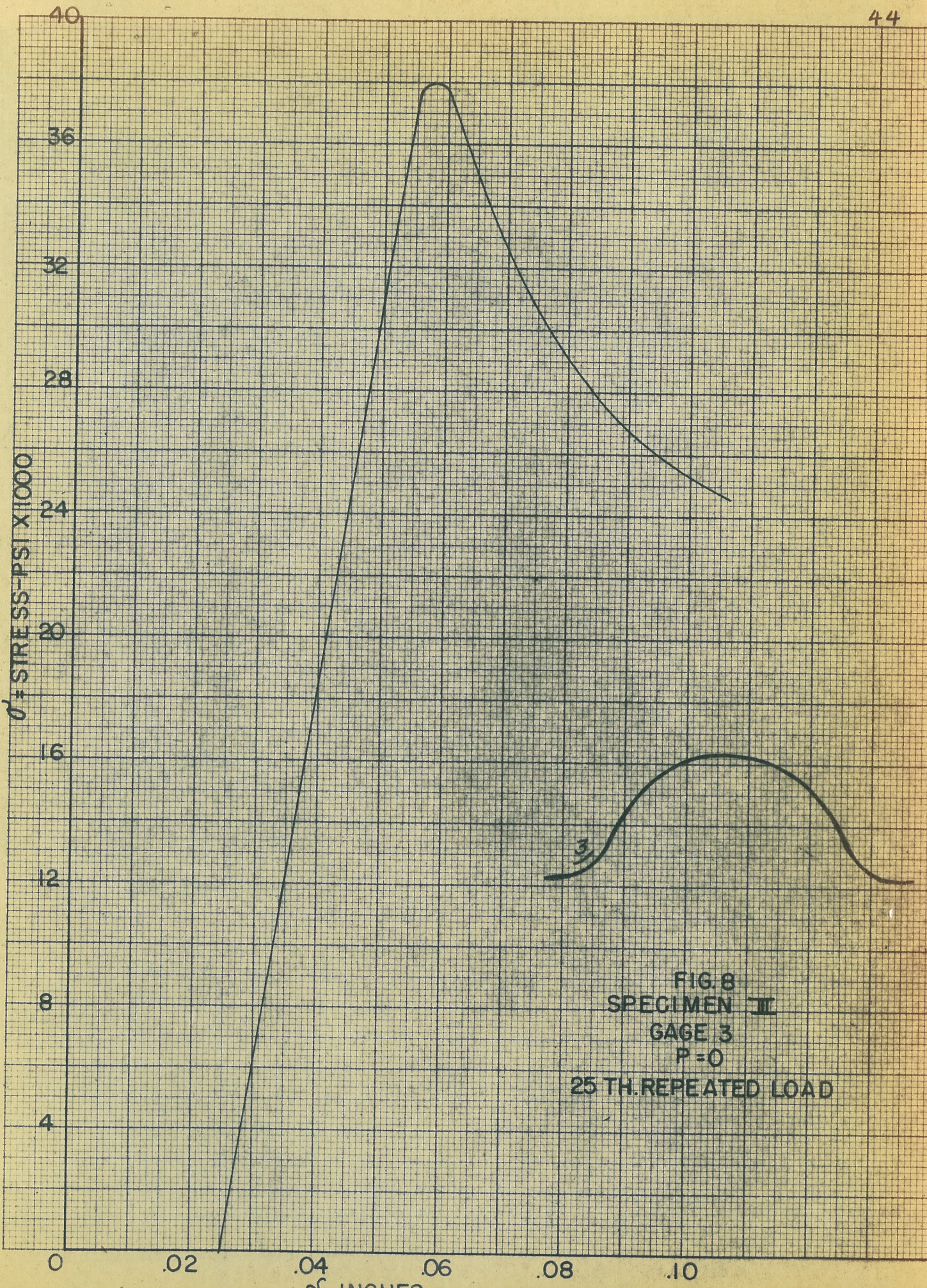


FIG. 8
SPECIMEN II
GAGE 3
P=0
25 TH. REPEATED LOAD

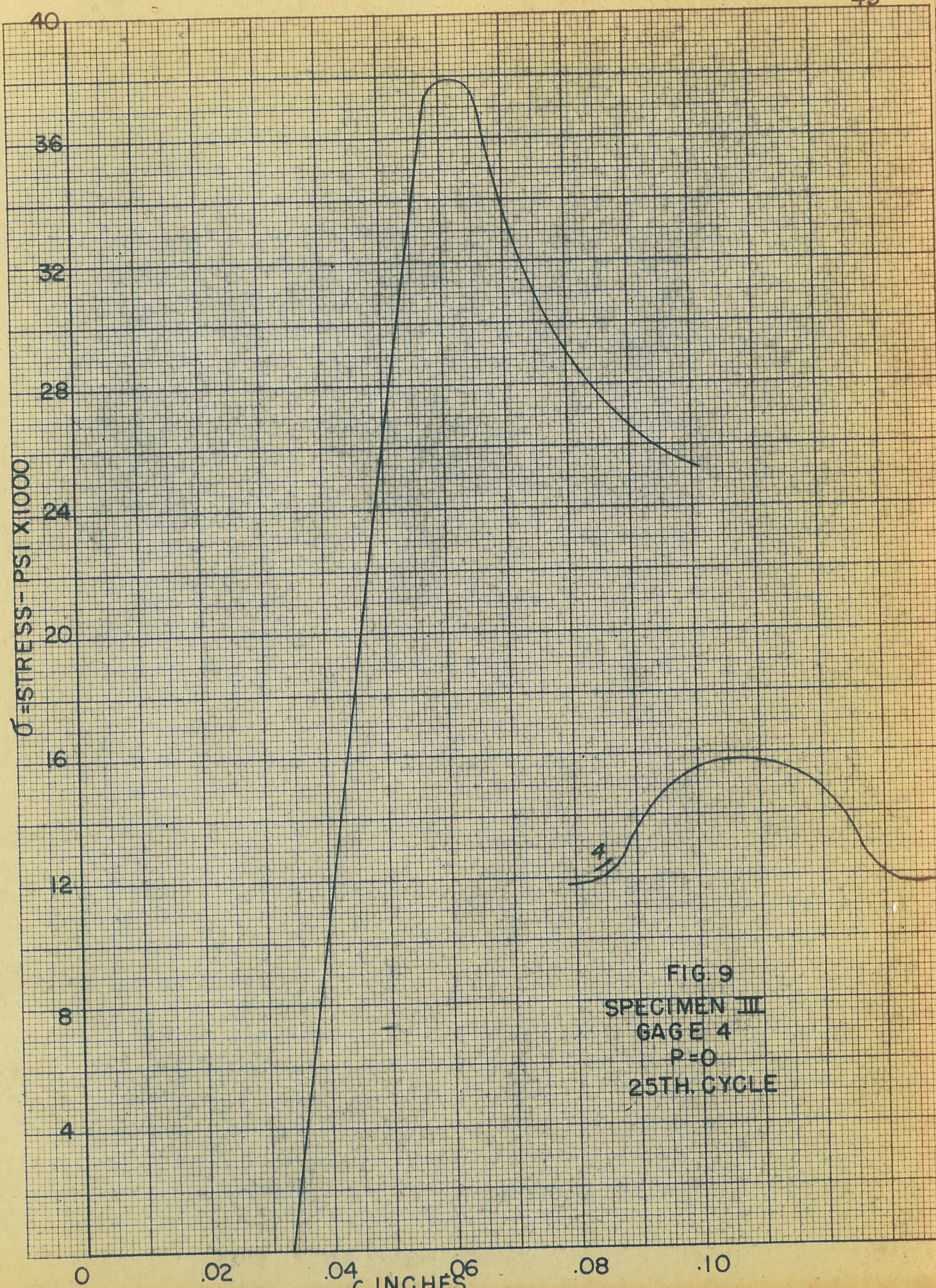


FIG. 9
SPECIMEN III
GAGE 4
P=0
25TH. CYCLE

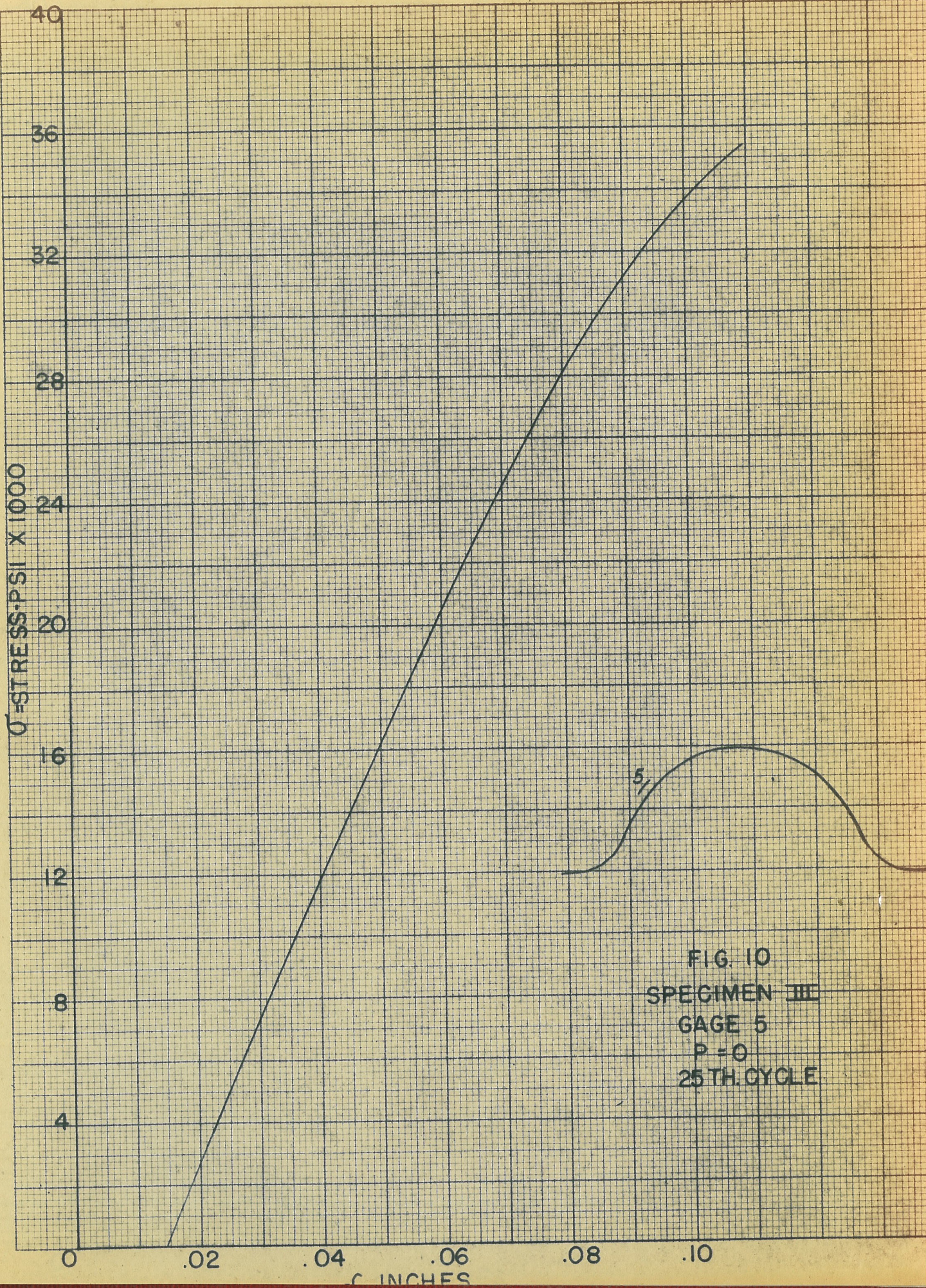


FIG. 10
SPECIMEN III
GAGE 5
P = 0
25TH CYCLE

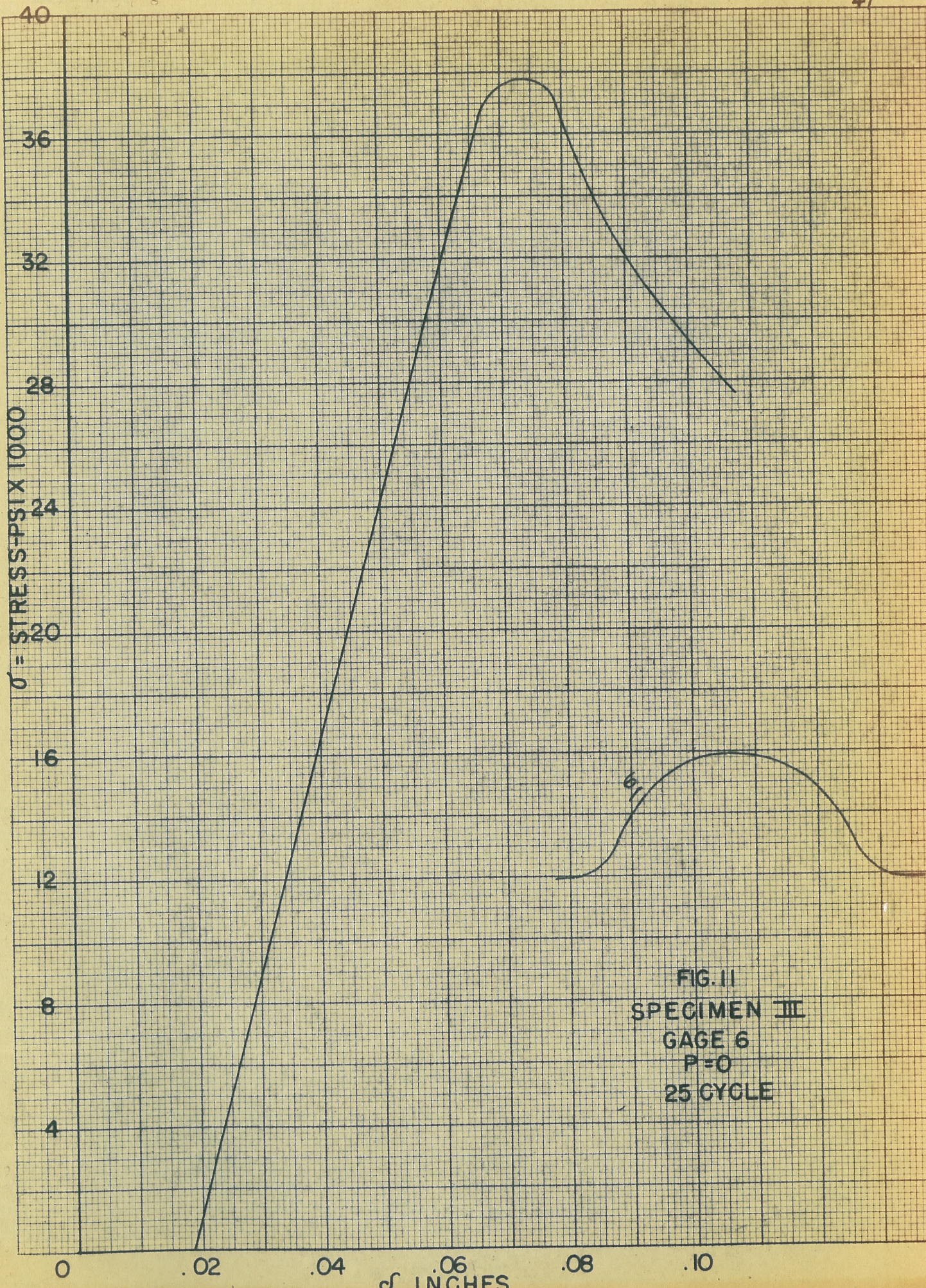


FIG. II
SPECIMEN III
GAGE 6
P=0
25 CYCLE

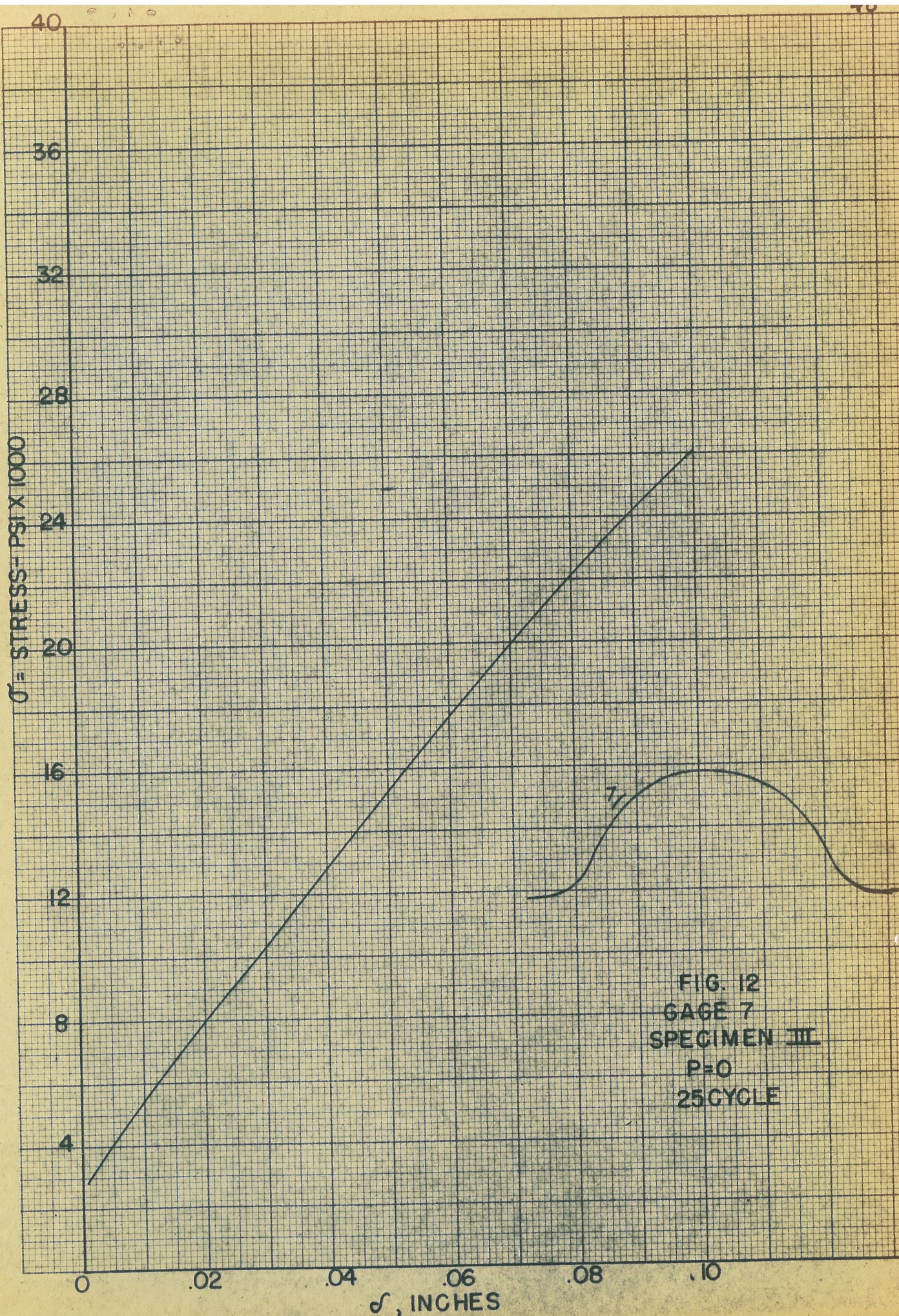


FIG. 12
 GAGE 7
 SPECIMEN III
 P=0
 25CYCLE

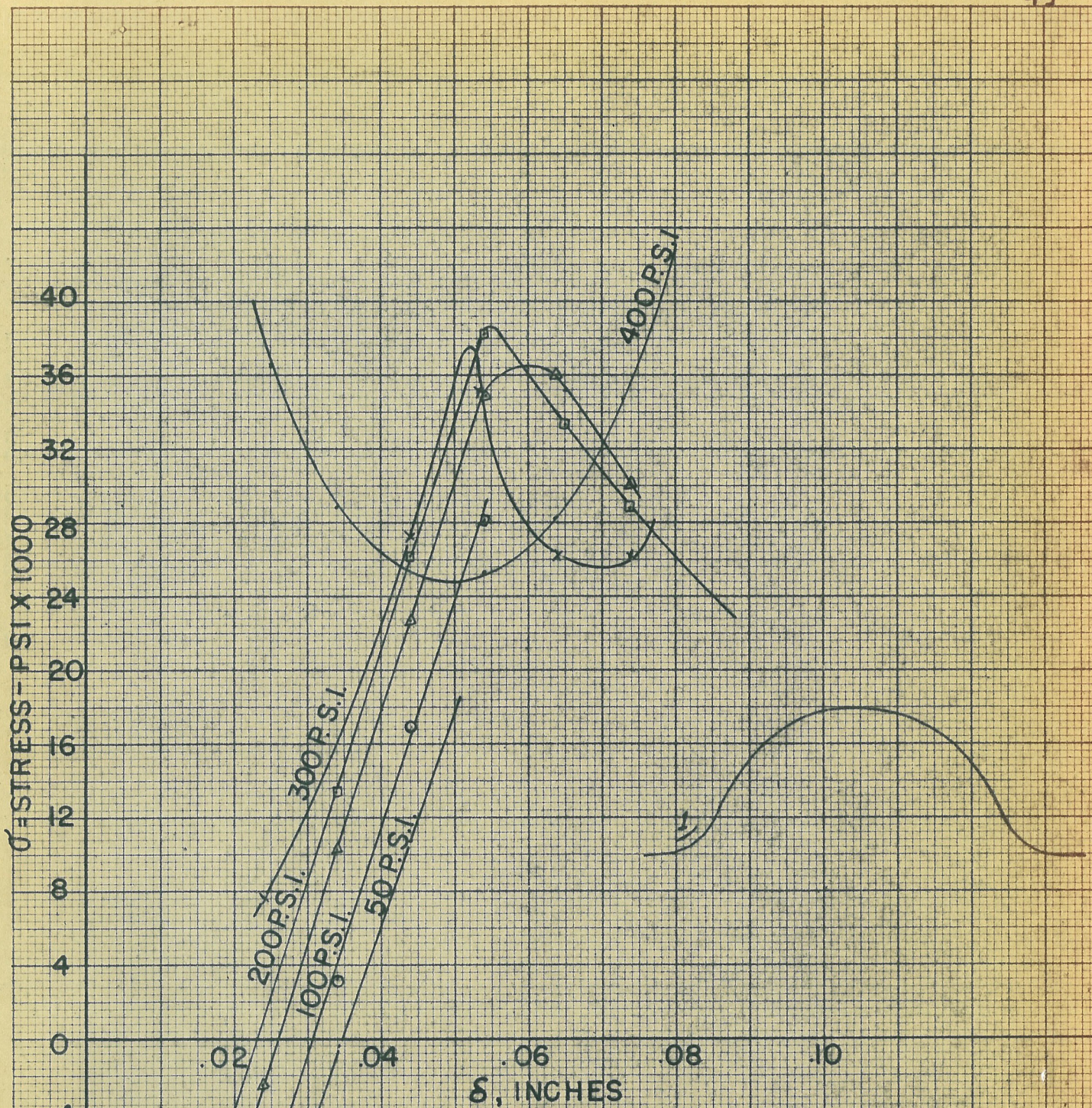


FIG. 13
SPECIMEN III
GAGE I
δ VARIED AS PRESS. HELD CONST.

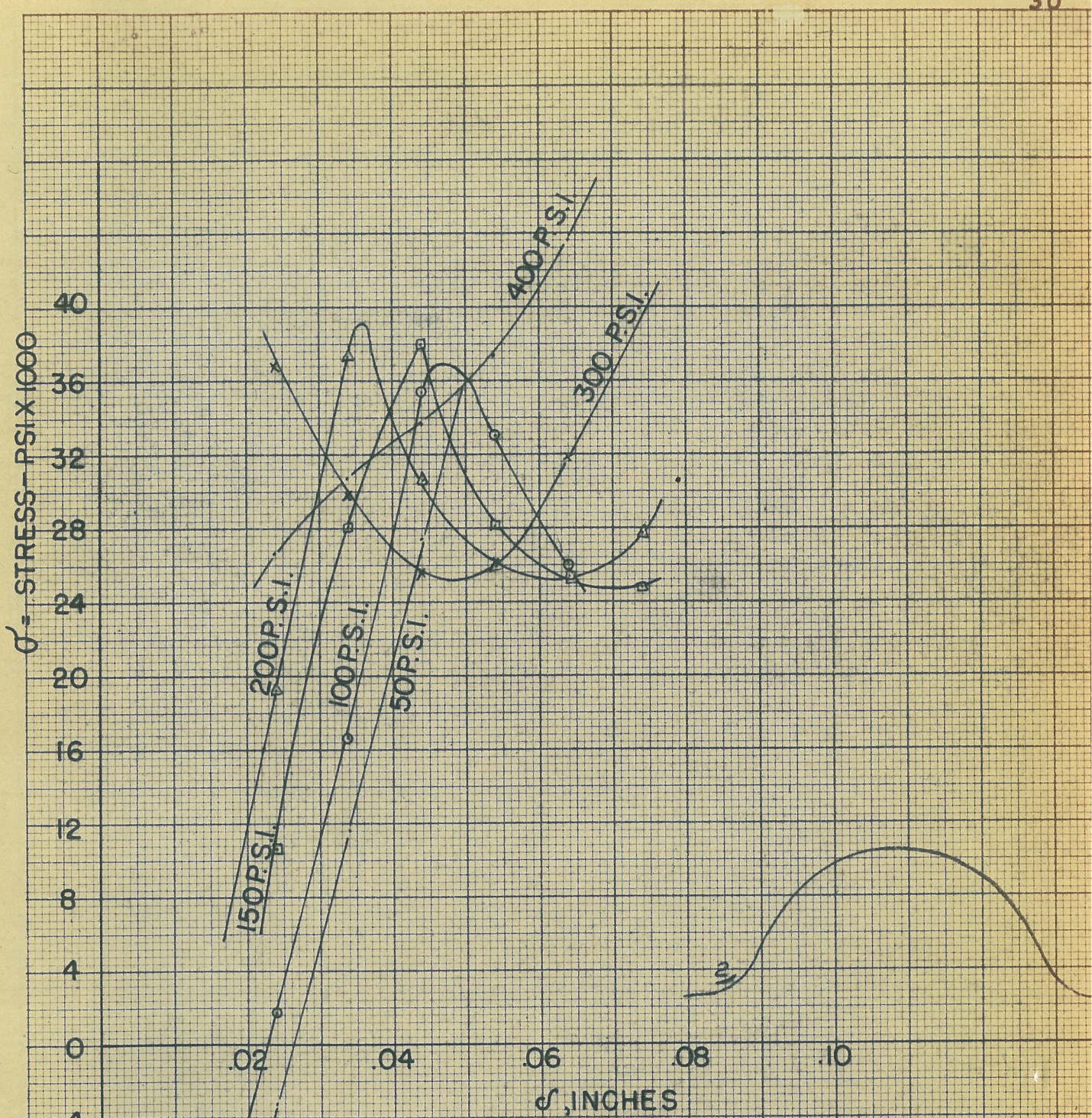


FIG. 14
 SPECIMEN III
 GAGE 2
 ϵ VARIED AT CONST. INT. PRES

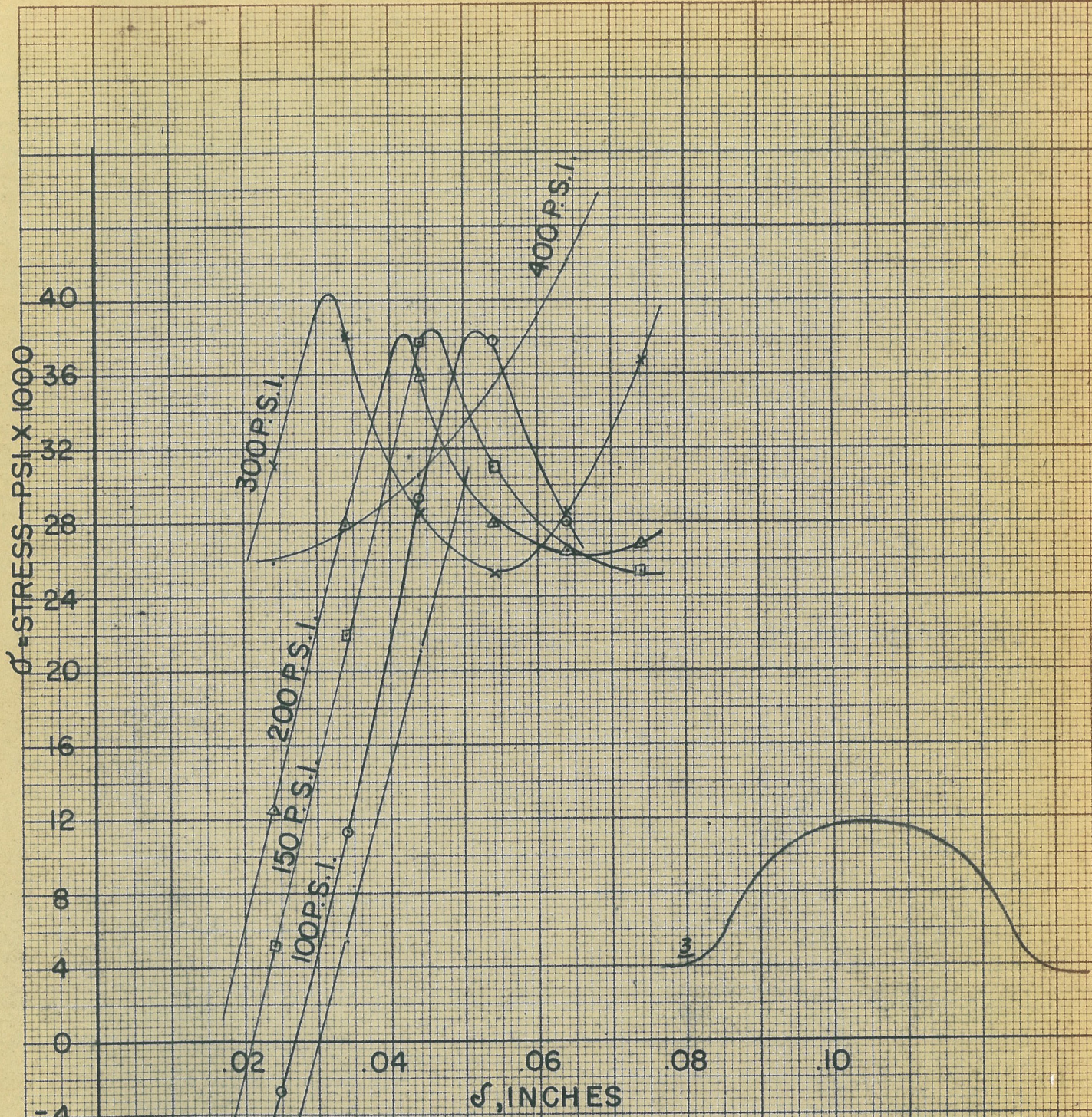


FIG. 15
SPECIMEN III
GAGE 3
ε VARIED AT CONST. INT. PRESS.

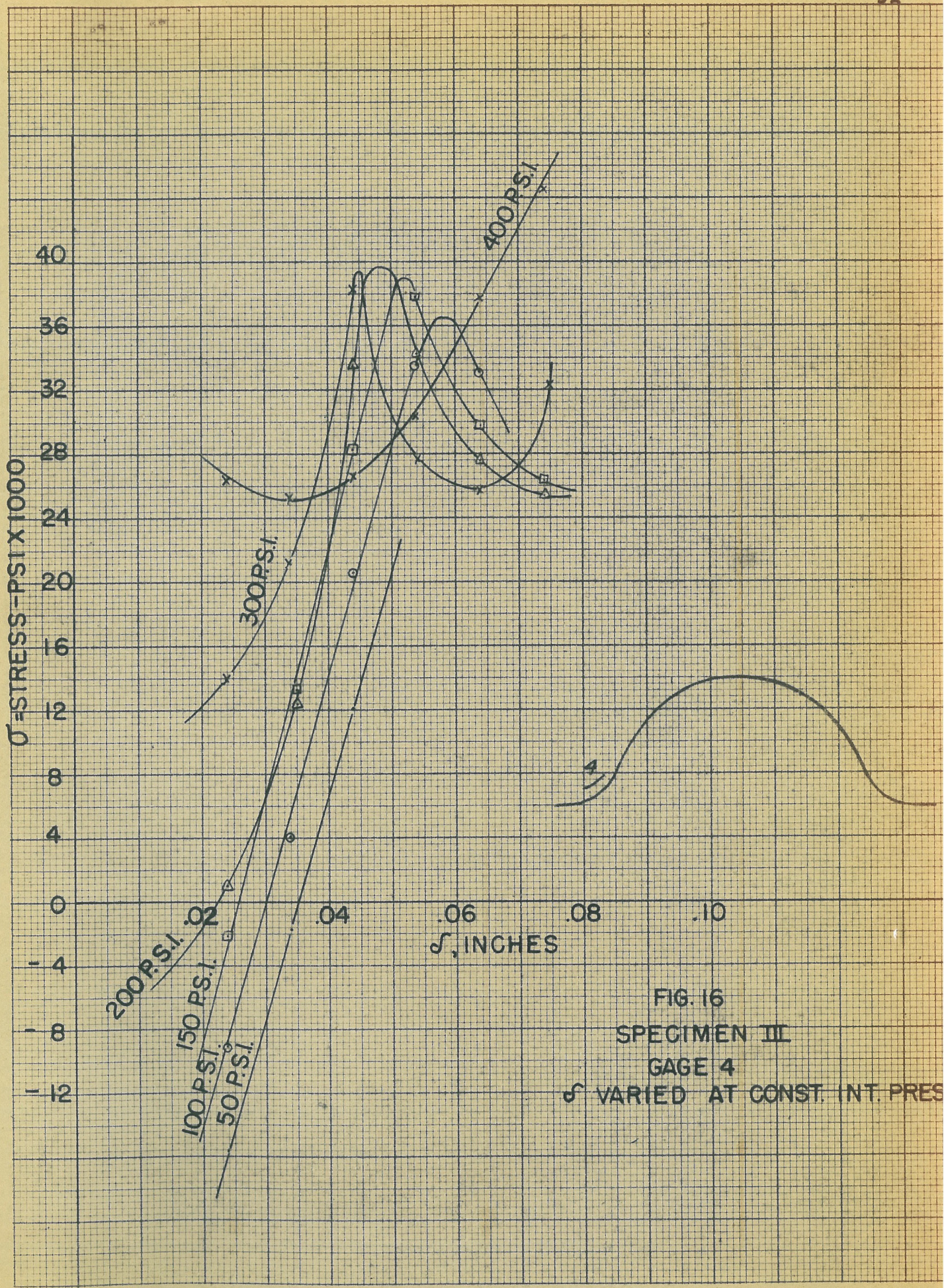


FIG. 16
SPECIMEN III
GAGE 4
 σ VARIED AT CONST. INT. PRES

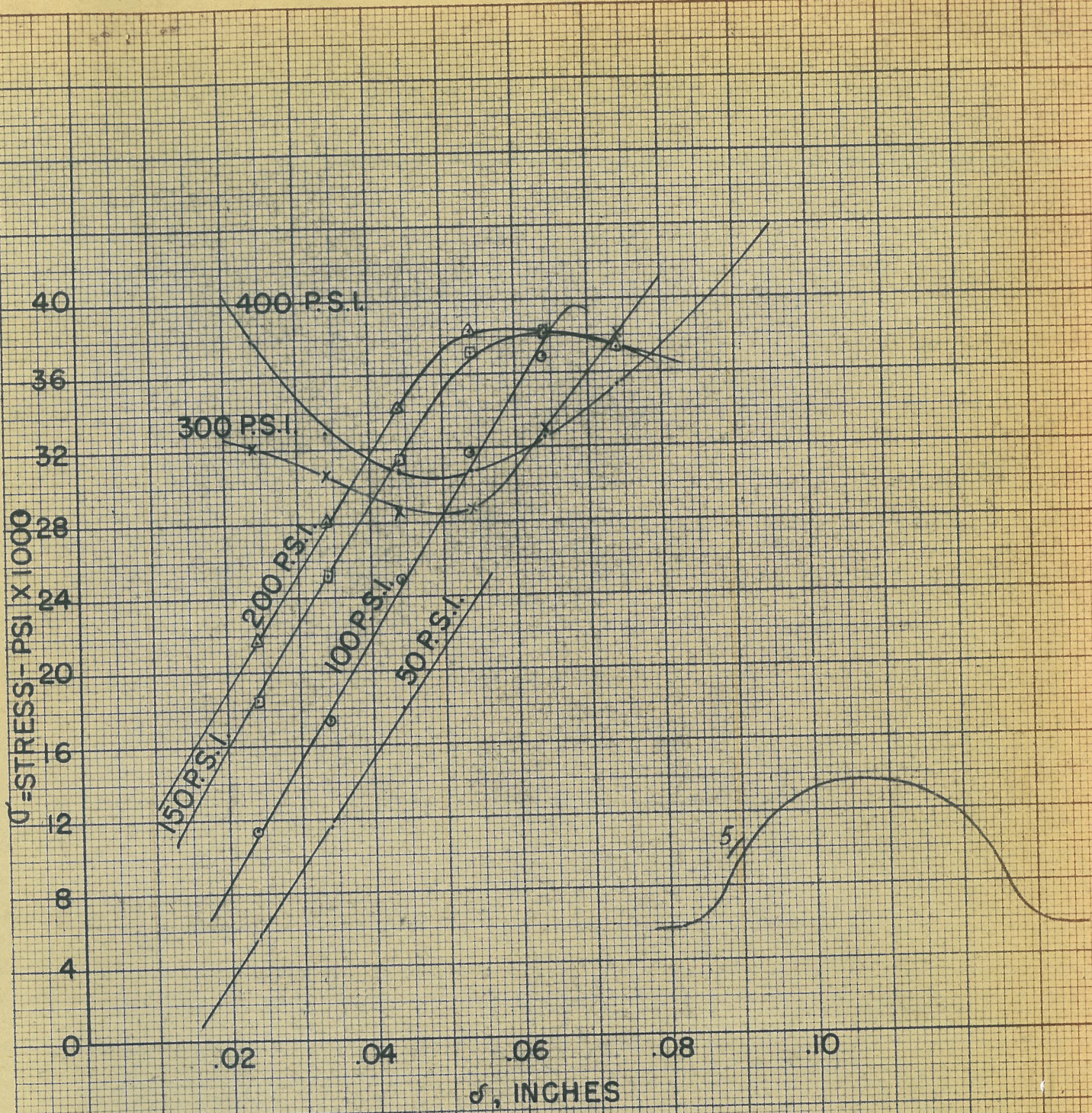


FIG. 17
SPECIMEN III
GAGE 5
 τ VARIED AT CONST. INT. PRES.

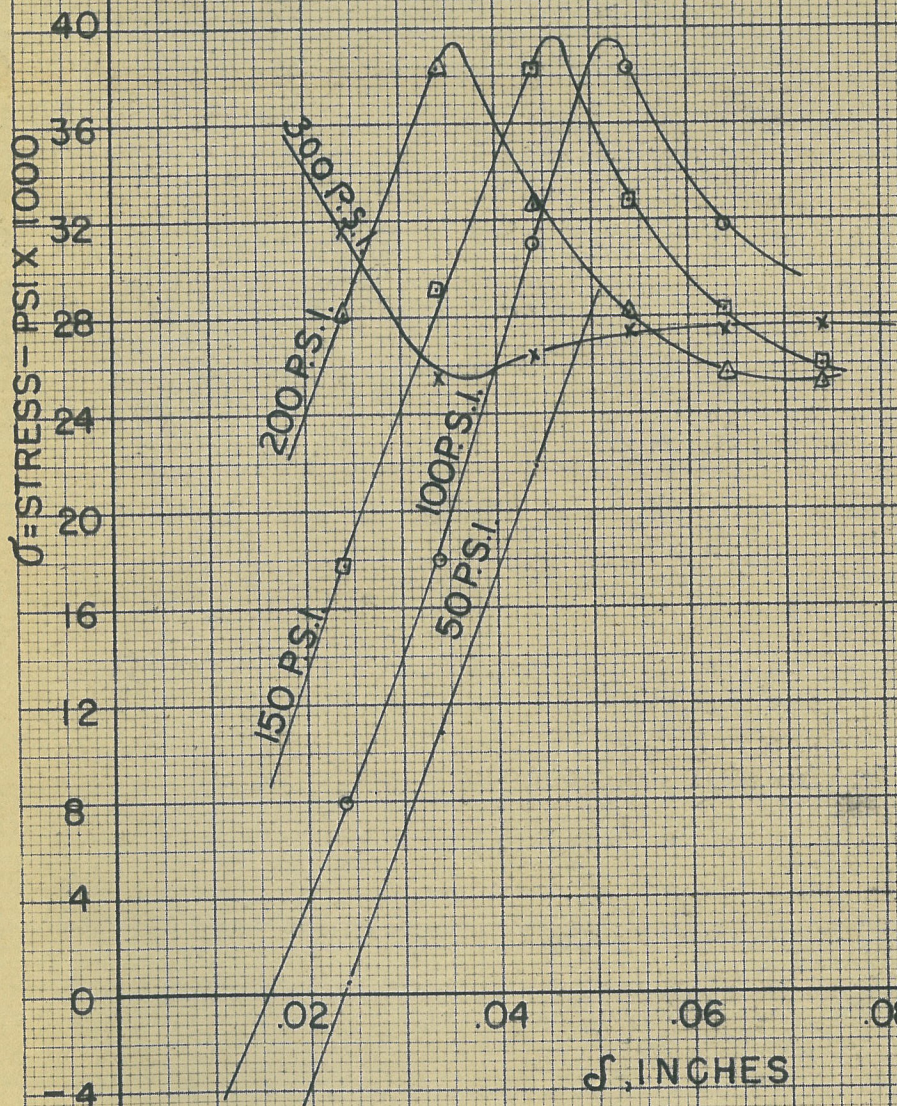


FIG. 18
SPECIMEN III
GAGE 6
 δ VARIED AT CONST. INT. PRESS.

61

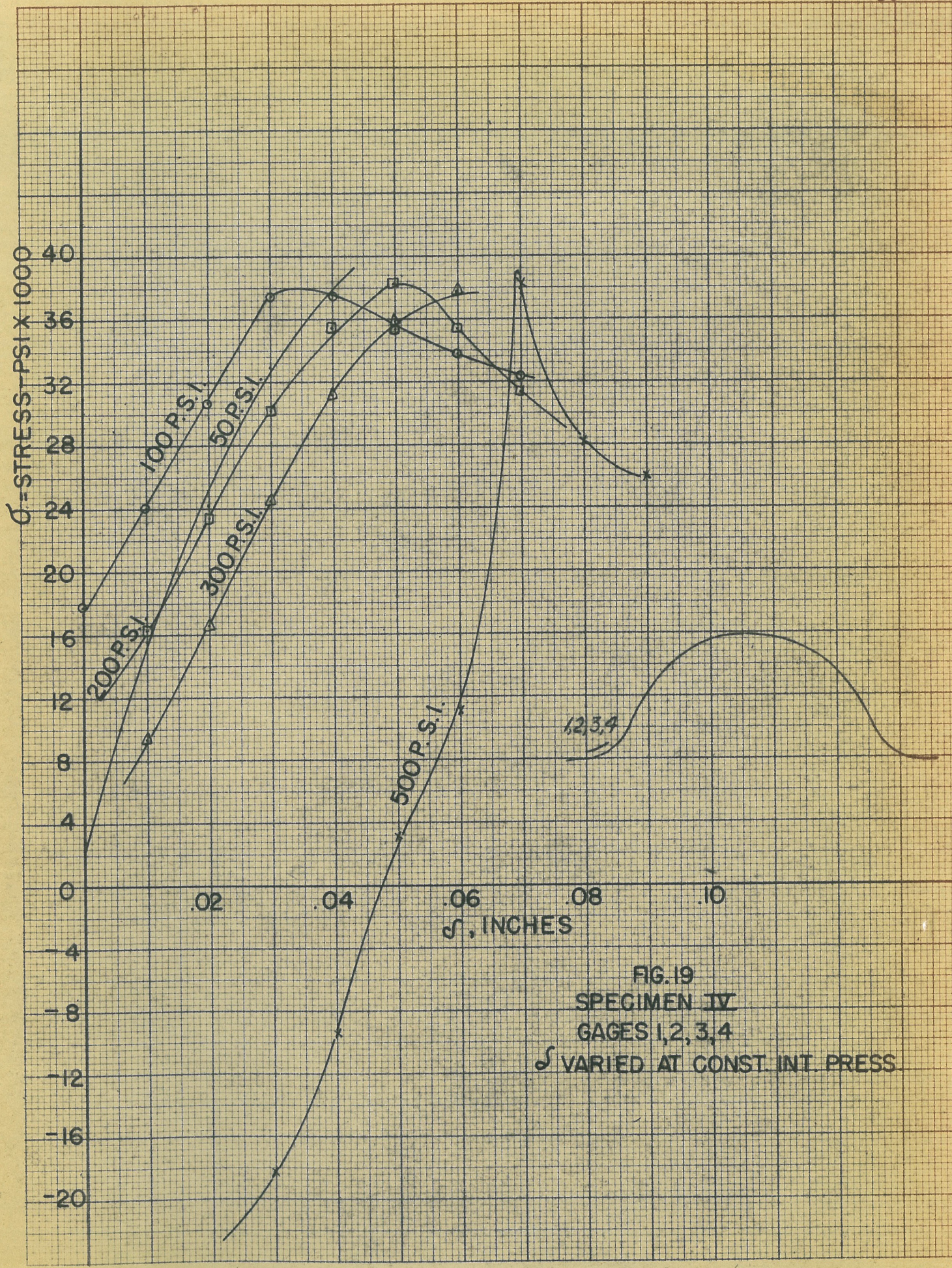


FIG. 19
SPECIMEN IV
GAGES 1,2,3,4
 ϵ VARIED AT CONST INT PRESS

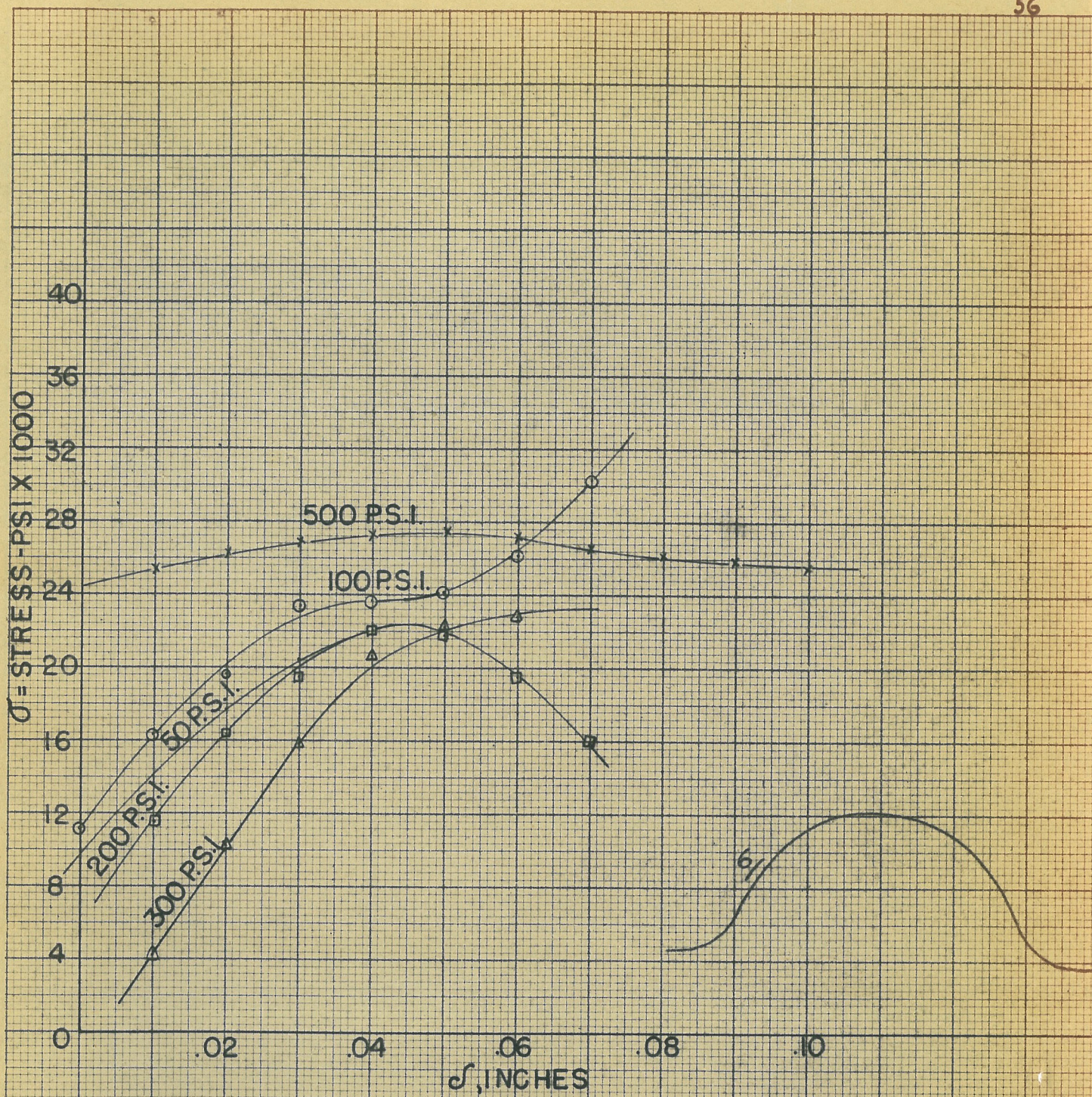


FIG. 20
SPECIMEN IV
GAGE 6
 ϵ VARIED AT CONST. INT. PRESS.

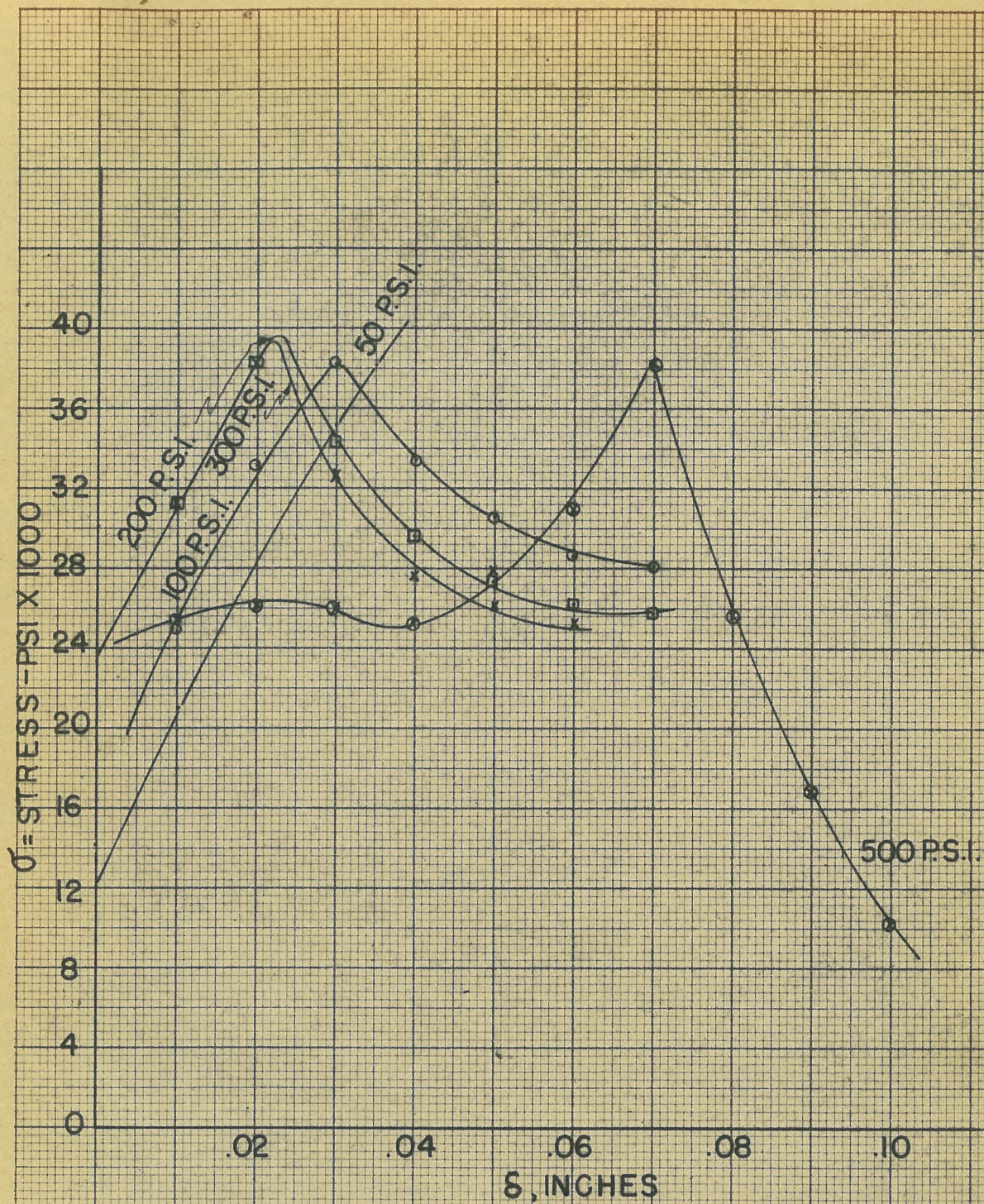
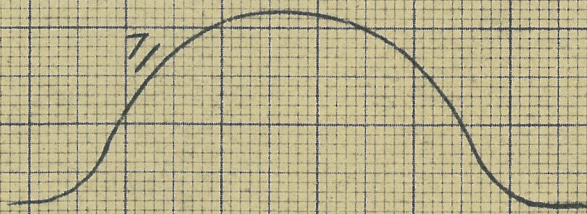


FIG. 21
 SPECIMEN IV
 GAGE 7
 σ VARIED, INT. PRESS. HELD CONST.



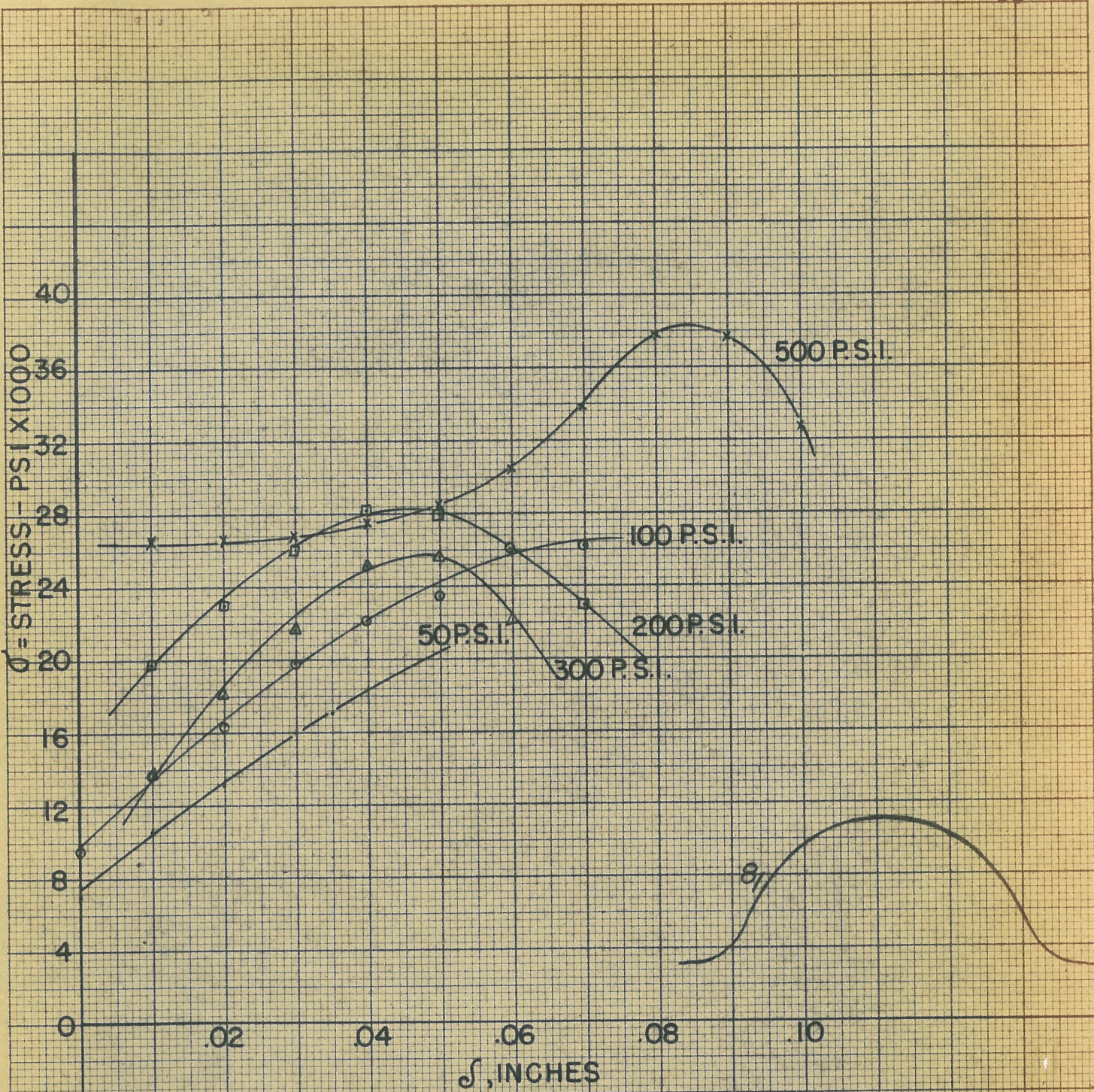


FIG. 22
 SPECIMEN IV
 GAGE 8
 γ VARIED AS PRESS. HELD CONST.

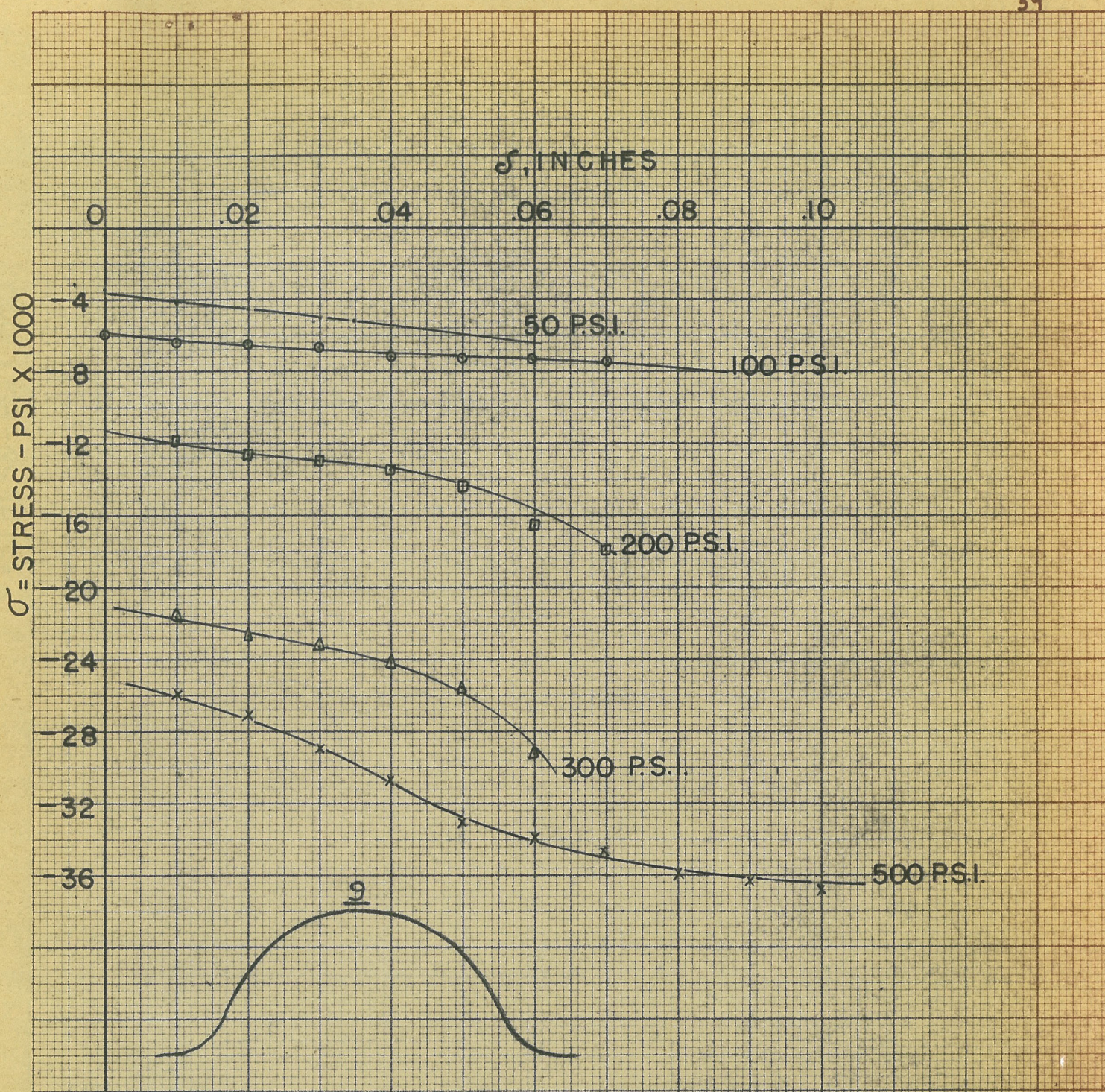


FIG. 23
SPECIMEN IV
GAGE 9
δ VARIED AS PRESS. HELD CONST.

σ = STRESS - PSIX 1000

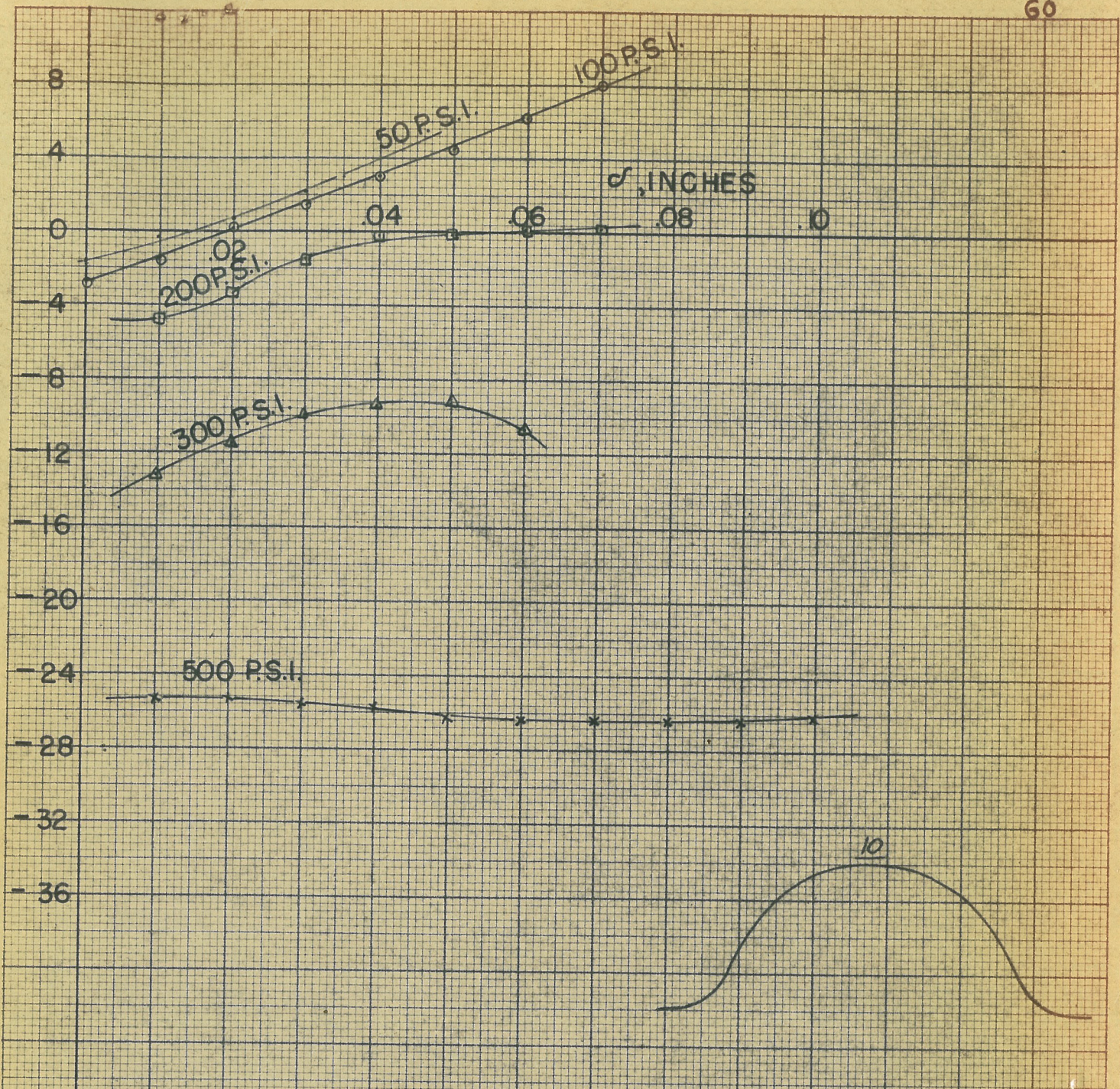


FIG. 24
 SPECIMEN IV
 GAGE 10
 ϵ VARIED AS PRESS. HELD CONST.

FIG. 25

